Materials Advances

ROYAL SOCIETY OF CHEMISTRY

REVIEW

View Article Online
View Journal | View Issue

Cite this: *Mater. Adv.*, 2021, 2, 64

Colorimetric and fluorometric probes for the optical detection of environmental Hg(II) and As(III) ions

Tapendu Samanta and Raja Shunmugam *

Received 19th July 2020,
Accepted 11th November 2020

DOI: 10.1039/d0ma00521e

rsc.li/materials-advances

Human exposure to Hg(II) and As(III) can lead to several physiological problems such as liver damage, kidney damage, lung cancer, skin cancer, motion disorder, brain damage, *etc.* To monitor and identify these harmful ions, throughout the years enormous effort has been put into the development of sensors. In this review, colorimetric and fluorometric chemical compounds (sensors) for Hg(II) (since 2015) and As(III) detection are described and discussed in detail. For Hg(II), sensors are divided on the basis of the compound's nature, such as heteroatom-based ligand-containing small molecules, rhodamine-based small molecules, reaction-based small molecules, and polymers. On the other hand, most As(III) ion sensors are based on H-bonding interactions.

1. Introduction

A highly polluted living environment for humankind is a result of modern globalization and industrialization, where water sources are the most affected part while water is the basic and essential ingredient of human life on earth. Heavy metals are one of the most effective pollutants among other sources. Metals with a high atomic number, high density, and which are poisonous at low concentrations are known as heavy metals.[1–3] Heavy metals are harmful due to their tendency to bioaccumulation. Heavy metals can enter the human body through food, drinking water, and air sources. Metals such as arsenic, cadmium, lead, nickel, mercury, chromium, cobalt, zinc, copper and selenium are familiar heavy metals. The accumulation of these metals in our resources is a major concern as many industries discharge their metal wastes into freshwater without any purification.[4,5]

Among the mentioned heavy metals, arsenic (As) and mercury (Hg) are the topmost candidates in the context of toxicity. The World Health Organization (WHO) and Environmental Protection Agency (EPA) have defined the permissible limits of concentrations for both mercury and arsenic.[6]

Arsenic poisoning in groundwater is a major concern in several parts of the world, such as Bangladesh, West Bengal, the western USA, Mexico, Chile, and Argentina.[7] Many electronic component manufacturing industries use trace amounts of arsenic combined with silicon for light-emitting diodes (LEDs) and other devices.[8] Although in some cases arsenic is used in drugs, chronic exposure can damage the human body. Long-term exposure and usage of arsenic-contaminated water can cause various health risks, such as kidney damage, liver damage, lung cancer, and skin cancer.[9–11] Arsenic can exist in −3 to +5 oxidation states, though the As(III) form is the most toxic to the environment and human health.[12] Due to such toxicity, the WHO set a limit of a safe arsenic (As) concentration in drinking water of 10 ppb.[13,14]

Mercury is another heavy metal that is famous for Minamata disease[15] and poisoning in Iraq.[16] Mercury can spread in water, soil, and air from many sources, such as coal plants, mercury lamps, gold production, thermometers, barometers, and caustic soda.[17] Fish is one of the major sources of mercury in humans.[18] Mercury exposure has several harmful effects on health, like kidney failure, motion disorder, and brain damage.[19–21] Methylation of mercury promotes lipid solubility and, as a result, it can easily penetrate biological membranes along with the blood–brain barrier to damage the central nervous system. To avoid the harmful effects of mercury, an upper limit for Hg has been set at 10 nM by the U.S. Environmental Protection Agency (EPA).[22]

The extent of toxicity for arsenic and mercury makes it necessary to monitor them in drinking water and different environmental sources with high selectivity and sensitivity. Techniques such as atomic absorption spectroscopy (AAS), inductively coupled plasma mass spectrometry (ICP-MS), atomic fluorescence spectrometry (AFS), high-performance liquid chromatography (HPLC), surface-enhanced Raman scattering, chromatographic techniques, hydride-generation atomic absorption spectroscopy (HG-AAS), and voltammetry studies are used for the detection of arsenic and mercury.[23–33] The above-mentioned techniques are well known for their detection ability in very low concentrations, but they need costly instrumentation and extensive sample preparation. Therefore, the development of simple, cost-effective, and rapid detection methods is very much needed for real-time and 'on-field'

Polymer Research Centre, Department of Chemical Sciences, Indian Institute of Science Education and Research, Kolkata, India. E-mail: sraja@iiserkol.ac.in

monitoring of industrial, environmental, and biological contaminated samples.

Among different methods, optical detection through changes in fluorescence or color are most advantageous due to their simple nature and low limit of detection.[34–37] Colorimetric sensors can be useful in the case of the naked eye and rapid detection of analytes without any prior set-up where fluorogenic probes can detect contaminants at the cellular level. Thanks to such advantages, fluorescent and colorimetric sensors have been developed throughout the last few decades for the detection of toxic elements.

To date, three reviews have reported which have provided collective information about various detection systems for environmental Hg^{2+}. These reviews discussed optical probes developed up to 2015.[38–40] Furthermore, there have been several reviews for arsenic detection based on the electrochemical method,[41] surface-enhanced Raman spectroscopy (SERS),[42,43] and nano-material systems.[44–46] However, to the best of our knowledge no review based on fluorogenic and chromogenic compounds for As(III) detection has been reported.

In this review, we discuss in detail fluorescent and colorimetric chemical sensors for mercury and arsenic detection. We have classified the sensors depending upon their chemical behavior, such as interaction-based ligand systems, reaction-based irreversible systems, and polymeric materials for a clear and general overview of available sensing materials that have been developed in recent years. Until 2015, there were not such extensive studies on cellular-level tracking of toxic ions. But the new trend of tracking toxic ions at the cellular level has emerged as an excellent technique for a better understanding of their effects on the biological system. Exclusive selectivity and high sensitivity along with cell imaging have become the better outcomes of the sensing field at the present time for mercury and arsenic. Also, many new strategies have been developed in the field of polymer research, where functionalized polymers with sensing moieties have overcome the solubility issue with respect to small molecules and have triggered an improvement in 'in-field' applications for the detection of toxic ions. We have tried to give an overall idea of new ways and new developments in mercury and arsenic detection systems based on typical fluorogenic and chromogenic probes.

2. Fluorescent and colorimetric sensors for Hg^{2+} detection

2.1 Heteroatom-based ligand-containing small molecules

Heteroatom-containing ligands associated with a chromogenic or fluorogenic moiety are excellent candidates for the detection of analytes. Ligand-based sensors have been developed over the years with desirable signals and effectiveness for the detection of Hg^{2+} ions in different contaminated sources. In this section we will discuss the formation of Hg–O, Hg–S, Hg–N, *etc.* bonds due to the interaction of Hg and a ligand to promote some change in color or emission as a detection signal.

In this regard, an *N*,*N*-bis(2-(pyridin-2-ylmethoxy)ethyl)aniline receptor containing a boron-dipyrromethene (BODIPY) molecule **1**[47] acts as a fluorescence 'turn-off' to 'turn-on' sensor for Hg^{2+} (Fig. 1). Here **1** can detect mercury in CH_3CN–water (1 : 1) medium with a limit of detection (LOD) of 1.81×10^{-7} M. In this case due to the presence of an *N*,*N*-bis(2-(pyridin-2-ylmethoxy)ethyl)aniline receptor along with BODIPY, the PET process is in the active mode which results in a fluorescence-off mode in the system. But the addition of Hg^{2+} stopped the photoinduced electron transfer (PET) process by interaction with the N and O atoms of the ligand which triggered the strong emission signal. All these observations made sensor **1** a highly selective and sensitive system for the detection of Hg^{2+} by the naked eye. A pyrene derivative **2**[48] formed a 1 : 2 complex with Hg^{2+} in 4-(2-hydroxyethyl)piperazine-1-ethanesulfonic acid (HEPES) buffer-CH_3CN (3 : 7, v/v, 10 mM buffer, pH = 7.4) medium (Fig. 1). Due to complexation, **2** showed an unusual red fluorescence and a change in color from yellow to orange along with a 36 nM LOD. The change in color as well as in emission is an advantage for **2**.

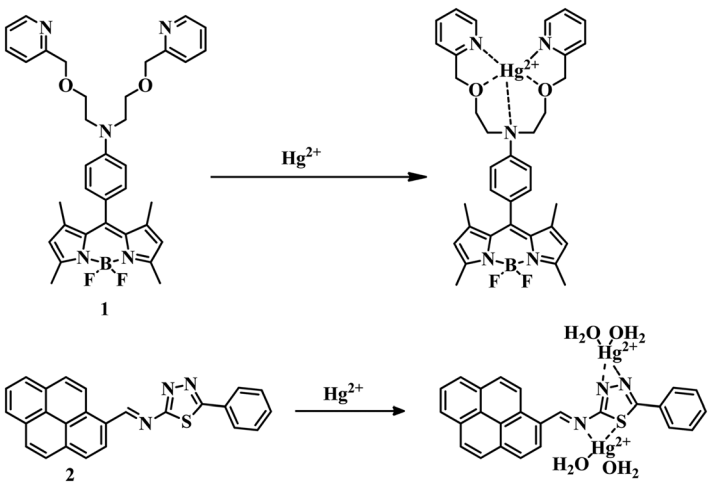

Fig. 1 The structures of **1** and **2**, and their proposed mechanisms of binding with Hg^{2+}.

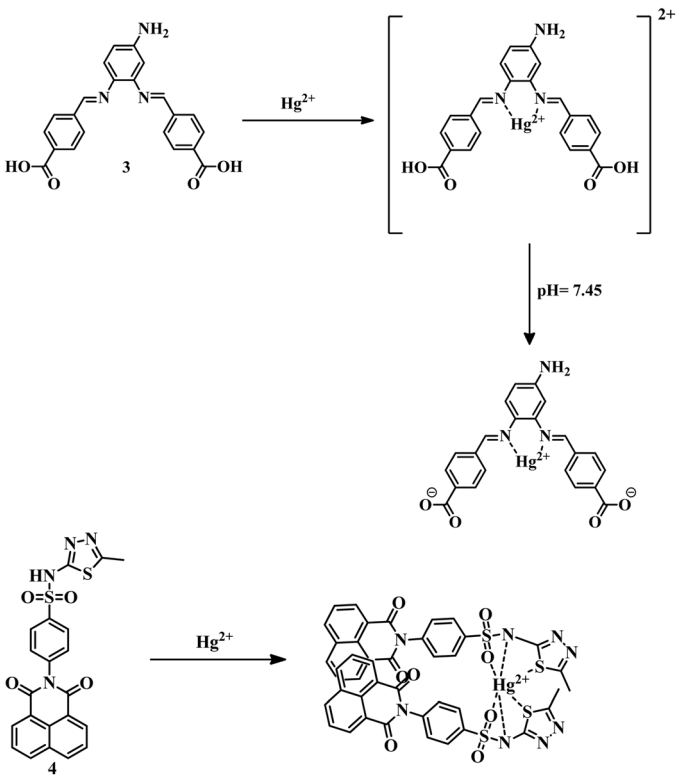

Fig. 2 The proposed structures and sensing mechanisms of **3** and **4**.

A Schiff-base **3**[49] synthesized from 4-nitro-*o*-phenylenediamine and 4-formylbenzoic acid showed interesting sensing phenomena for the detection of Hg^{2+} in DMF–water (2 : 3) medium with an LOD of 0.061 μM. Initially, **3** showed green fluorescence, though upon addition of mercury at pH 7 the fluorescence was quenched, but at pH 7.45 fluorescence was turned on again (Fig. 2). The whole phenomenon was described as due to the reduction of intramolecular charge transfer (ICT) caused by the formation of a strong 5-membered ring between Hg^{2+} and two imine nitrogens at pH 7 and again the introduction of ICT with increasing pH. Due to this interesting behavior of **3** in physiological pH, it has been used in cell imaging studies to extend their application. Sensor **4**[50] also exhibits a ratiometric emission changing phenomenon due to the binding of heteroatoms of 1,8-naphthalimide-sulfamethizole compound with Hg^{2+} in DMSO–water (1 : 99) medium with an LOD 14.7 nM. Binding of Hg^{2+} with $–SO_2$ and the thiadiazole ring of the sulfamethizole segment of **4** leads to aggregation-induced emission enhancement (AIEE) which is responsible for the selective detection of mercury (Fig. 2).

Tetraphenylethene derivatives are known for their aggregation-induced emission property. Using this as an advantageous property, sensor **5**[51] has been developed by the reaction of 2-(aminooxy)acetic acid and 4-(1,2,2-triphenylvinyl)benzaldehyde. With the addition of mercury to sensor **5** in ethanol–water (3 : 7) medium, the –CH═N and –OH groups coordinate with Hg^{2+} (Fig. 3) and form an aggregate to give a distinct emission with a low LOD of 45.4 nM. BODIPY derivatives are known to have excellent chromophore photochemical and thermal stability, and salen is an excellent ligand system due to its effective coordination behavior with an electron-deficient Lewis-acid (metal center).[52,53] Sensor **6**[54] was designed by the combination of the two above-mentioned advantageous segments for the detection of Hg^{2+}. Sensor **6** selectively detected Hg^{2+} among other metal ions by complexation in MeCN–H_2O (v/v, 1 : 1, HEPES 10 mM, pH = 7.4) medium with an LOD of 1.21 μM (Fig. 3). In this particular case, metal-induced intramolecular charge transfer is the reason behind the change in color from colorless to pink to detect Hg^{2+} selectively and sensitively.

For biimidazole push–pull dye, sensor **7**[55] coordinates with Hg^{2+} through the thiophene unit (Fig. 4) and stopped the charge transfer process to change the color to colorless from yellow in a CH_3CN–water (1 : 1) mixture with an LOD of 32.8 ppb. With a combination of thiosemicarbazone and 4-(diphenylamino) benzaldehyde, sensor **8**[56] can detect Hg^{2+} in DMSO/Tris–HCl (8 : 2, v/v, pH = 7.0) medium. Hg^{2+} can bind with the sulfur of thiocarbonyl and the nitrogen of the imine group of **8** (Fig. 4) to induce a chelation-enhanced fluorescence quenching (CHEQ) effect. This fluorescence turn-off sensor **8** can detect Hg^{2+} up to a low concentration of 3.11×10^{-8} M. Sensor **9**[57] is a coumarin–thiol based receptor that detects Hg^{2+} in a CH_3CN–water (3 : 2, v/v, pH = 7) mixture in both colorimetric and fluorometric fashion with an LOD of 5.01×10^{-8} M. In this case binding of Hg^{2+} with –SH, N of the imine group, and the –C═O group of the coumarin unit of **9** (Fig. 5) induce a color change as well as change in fluorescence. This dual-sensing nature makes **9** a good candidate for mercury detection.

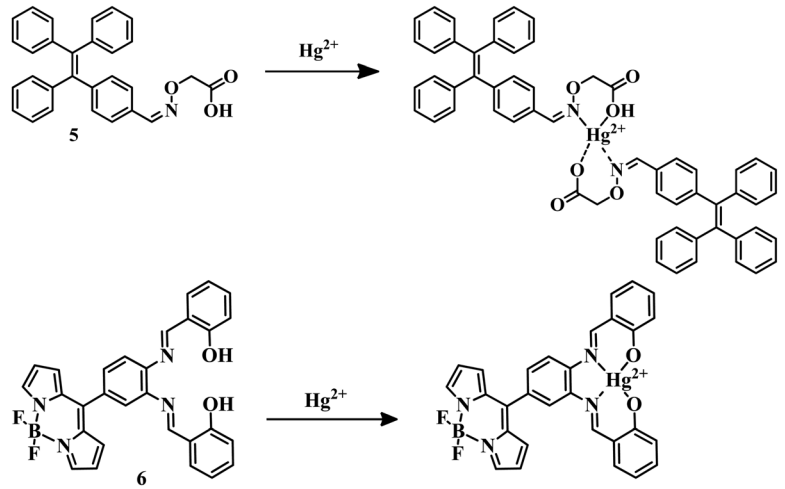

Fig. 3 The chemical structures and proposed mechanisms of sensing of **5** and **6**.

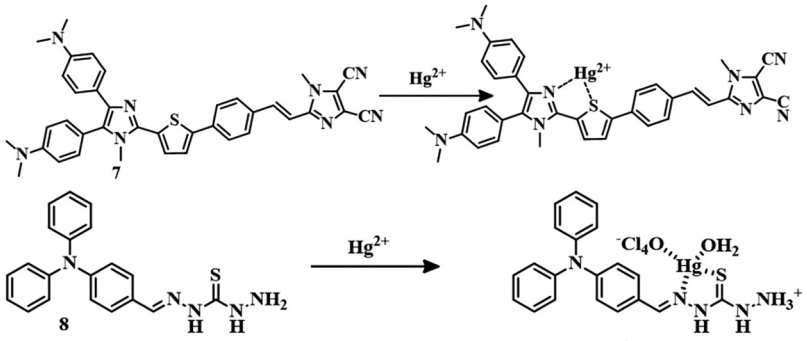

Fig. 4 The chemical structures and proposed binding modes with Hg^{2+} of **7** and **8**.

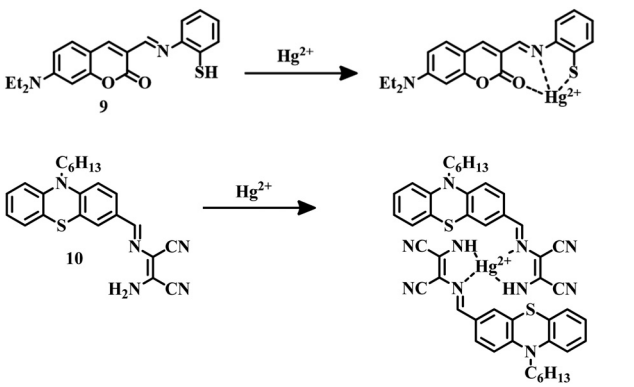

Fig. 5 The chemical structures of **9** and **10** along with their proposed sensing mechanisms.

Phenothiazine-based sensor **10**[58] was designed to detect Hg^{2+} in an ethanol–water (6 : 4, v/v) mixture with an LOD of 17.8 nM. Complexation of Hg^{2+} diaminomalenonitrile moieties of **10** (Fig. 5) inhibits the original ICT process; as a result, quenching of fluorescence and a change in color are observed. With this fluorescence change property, **10** can track cellular Hg^{2+} successfully. Receptor-based sensing models have emerged as a useful tool for the development of Hg^{2+} sensors. A sulfonamide group containing an unnatural peptide receptor with cyanostilbene-based ratiometric fluorogenic probe **11** has been developed.[59] It binds with Hg^{2+} in such a fashion that it can form an aggregate which is red-emissive (Fig. 6). Sensor **11** is highly selective towards Hg^{2+} in an aqueous buffered solution (10 mM HEPES, pH = 7.4) with an impressive detection limit of 65 nM. This red-emissive nature of **11** is useful for imaging of HeLa cells with Hg^{2+} contamination.

Macrocycles containing sulfur atoms are capable of capturing Hg^{2+}. Also, if the BODIPY unit can be functionalized with receptors in the 3 and 5 positions, then the recognition can induce a variation in both emission and absorption. Combining these facts, sensor **12**[60] was developed where *N*-phenyl-1-aza-4,13-dithia-7,10-dioxacyclopentadecane is attached to the 3 positions of the BODIPY unit (Fig. 6). This BODIPY derivative (**12**) can detect Hg^{2+} in CH_3CN–water (5 : 95, v/v) medium by a color change as well as turn-on mode of emission change with an LOD of 99 ppm. The design of a fluorescent probe can detect an analyte depending upon different phenomena like PET, FRET, ICT TICT, *etc.* for the output emission signal. 4-(Methylthio)-2-oxo-2*H*-pyrano[3,2-*c*]julolidine-3-carbonitrile derived sensor **13**[61] is a twisted intramolecular charge transfer

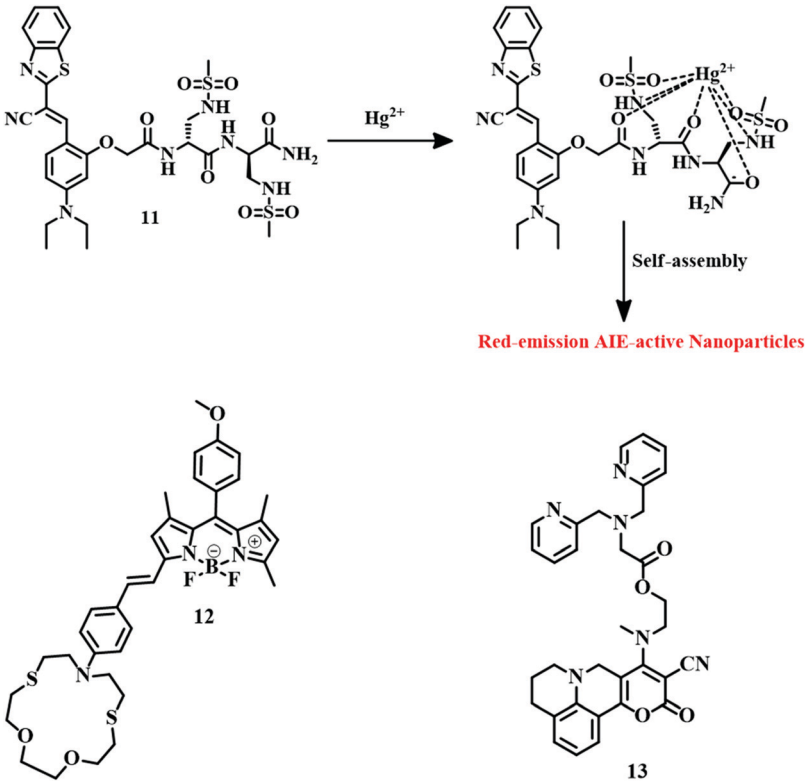

Fig. 6 The chemical structures of **11**, **12**, and **13** with the proposed mechanism of sensing for **11**.

(TICT) active fluorophore, where dipicolyl amine acts as a chelator to bind Hg^{2+} (Fig. 6). The sensing behavior of **13** has been studied in a methanol–HEPES buffer (7 : 3, v/v, pH = 7.2) medium. Sensor **13** detects Hg^{2+} in a ratiometric fashion by changing the emission from red to green with an excellent detection level of 5.7×10^{-9} M along with tracking of Hg^{2+} in the MCF-7 cell line. Binding with a dipicolylamine unit of **13** with Hg^{2+} restricts the TICT activity which is responsible for the drastic change in emission signal.

Aggregation induced emission (AIE)-based fluorogenic probes are very useful due to their unique fluorescence phenomenon. The tetrathenylethene unit is a well-established moiety for designing AIE-active molecules. Cationic AIE-active sensor **14**[62] consists of tetraphenylethene and quinoline units, and can detect Hg^{2+} by a different method. Initially, **14** showed red fluorescence in aqueous solution (containing 1% DMSO) due to aggregation, but the emission was quenched due to the addition of I^- to it. This I^--containing sensor **14** system can now act as an Hg^{2+} sensor. Addition of Hg^{2+} to the **14**–I^- system turns on the red emission again. By this process, **14** can be used as a turn-on fluorescence sensor for Hg^{2+} with a detection limit of 591.9 nM. Another AIE-active sensor **15**[63] is developed by the conjugation between tetraphenylethene and pyrido[2,3-*b*]pyrazine units. Sensor **15** has an excellent AIEE phenomenon itself. In the presence of Hg^{2+} in the acetonitrile solution sensor, **15** changed its emission color from red-orange to colorless with a moderate LOD of 7.46×10^{-6} M. The chemical structure of sensors **14** and **15** are depicted in Fig. 7.

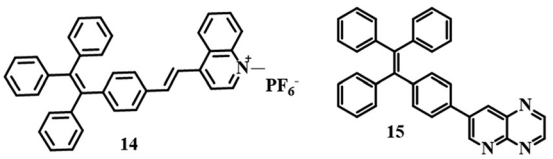

Fig. 7 The chemical structures of sensors **14** and **15**.

The 8-hydroxyquinoline based sensor **16** was successfully applied for the recognition of Hg^{2+} (Fig. 8).[64] In a solution of MeOH–water (1 : 4, v/v), fluorescence quenching was observed for Hg^{2+} with a simultaneous change in emission from blue to colorless. This is a typical example of a turn-off fluorescent sensor where complexation between the sensor and the analyte is responsible for fluorescence quenching.

Fluorescein as a fluorophore is widely used due to its high molar extinction coefficient, high quantum yield, and strong absorbance along with strong emission signals in the visible range.[65–67] Sensor **17**[68] is a fluorescein dithia-cyclic skeleton

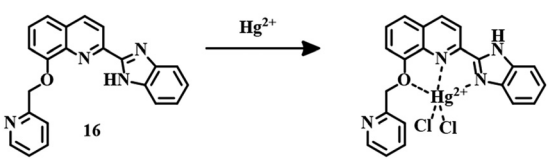

Fig. 8 The chemical structure of **16** and the proposed sensing mechanism.

which show selective detection ability for Hg^{2+} in an MeOH–Tris–HCl (95 : 5, v/v, pH = 7.2) medium. Upon interaction with Hg^{2+}, a drastic color change from yellow to orange was observed along with quenched fluorescence due to the inherent quenching property of mercury (Fig. 9). Another sensor **18**,[69] a Schiff base receptor of fluorescein–phenylalaninol conjugate has been successfully applied for the detection and removal of Hg^{2+}. The addition of Hg^{2+} to **18** in aqueous medium changed the color from yellow to pink with quenching of the fluorescence of the system. Binding of Hg^{2+} with the –CH═N and –OH groups is responsible for the quenching of fluorescence as well as color (Fig. 9). Sensor **18** has impressive LODs of 1.65 μM and 0.34 μM, as calculated from absorption and fluorescence studies, respectively. Another fluorescein-derived chemosensor **19** has been reported for the detection of Hg^{2+}. Sensor **19**[70] is a fluorescein hydrazide coupled 2-(pyridine-2-ylmethoxy)-naphthalene-1-carbaldehyde moiety which exhibited excellent selectivity and sensitivity towards Hg^{2+} in buffer solution (pH = 7.2, HEPES buffer). Hg^{2+}–induced spirolactam ring-opening of the fluorescein moiety is the reason behind the drastic enhancement in fluorescence (Fig. 9). An LOD of 1.24 μM and the ability to track Hg^{2+} at the cellular level make sensor **19** a good candidate in the area of mercury detection.

Excited-state intramolecular proton transfer (ESIPT)-active molecules are advantageous due to their excellent photostability, large Stokes shift, and unique emission properties. Naphthalene-derived sensor **20**[71] is an ESIPT-active probe that has been able to detect Hg^{2+} in CH_3CN–water (9 : 1, v/v, pH = 7.0, HEPES buffer) medium in a fluorescence on to off fashion accompanied by a drastic change in color from colorless to yellow. The interaction between the N and –OH groups of **20** and Hg^{2+} stopped the ESIPT process, resulting in fluorescence quenching (Fig. 10).

Terpyridine is a good chromophore that can be introduced to design colorimetric chemical sensors for metal ions. Sensor **21** is a colorimetric fluorescent probe, a combination of a terpyridine unit as a fluorescent moiety and three pyridine rings with ether linkers as receptors (Fig. 10). Sensor **21**[72] is a typical ratiometric fluorescent sensor for Hg^{2+} in aqueous medium by changing the fluorescence from blue to green with an LOD of 0.138 ppm. Initial blue fluorescence is due to weak ICT generated from the terpyridine segment. But after the strong complexation of Hg^{2+} by the receptor, the PET process becomes the driving force for the change in emission color to green. Due to this colorimetric fluorescence change, sensor **21**

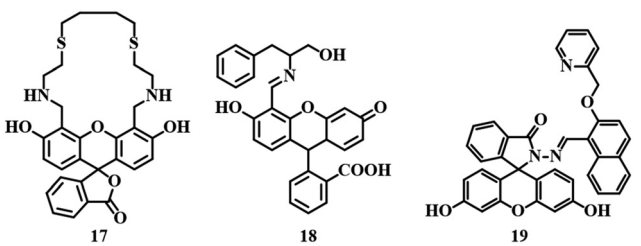

Fig. 9 The chemical structures of sensors **17**, **18**, and **19**.

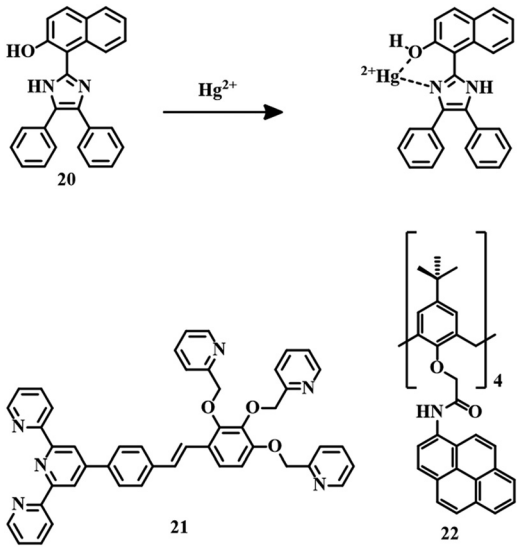

Fig. 10 The chemical structures of sensors **20**, **21**, and **22**, and the proposed sensing mechanism of sensor **20**.

can be coated on filter paper as paper strips, for the detection of the contaminant in various water sources with the naked eye.

Calix[4]arene-based fluorescent sensing probes are a combination of two parts, *i.e.*; an ionophore that is responsible for the analyte interaction and a fluorogenic moiety responsible for signal generation. Sensor **22**[73] is an example of a calix[4]arene-based probe where pyrene is used as a signaling unit (Fig. 10). Sensor **22** can detect Hg^{2+} selectively in CH_3CN–HEPES (6 : 4, v/v, pH = 7.2) medium with an excellent detection limit of 2.94×10^{-9} M. Complexation between Hg^{2+} and the carbonyl groups of the amide linkages of **22** is the reason behind the fluorescence quenching.

Naked-eye detection of analytes has its uses for cost-effectiveness and simplicity. Sensor **23**[74] is an NBD-based chemosensor (Fig. 11) which detects Hg^{2+} in a methanol–water (1 : 1) mixture by changing the color of the solution from pale yellow to pink with a detection limit of 4.7×10^{-7} M. The formation of a

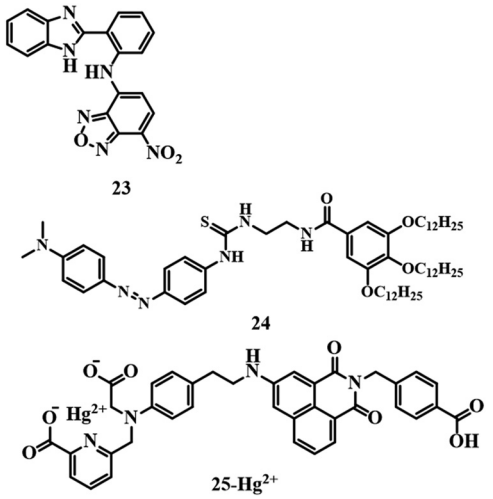

Fig. 11 The chemical structures of **23**, **24** and **25**–Hg^{2+}.

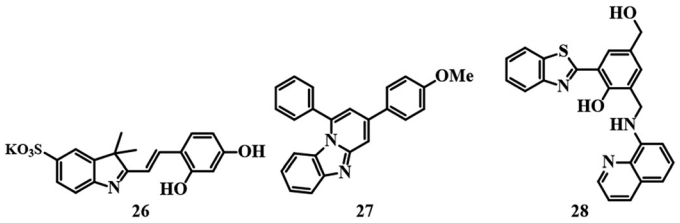

Fig. 12 The chemical structures of **26**, **27**, and **28**.

complex by interaction between **23** and Hg^{2+} triggered the intramolecular charge transfer (ICT) process; as a result, a pink color was observed. Another colorimetric sensor **24**,[75] an azobenzene gelator, acts as a multianalyte detection system (Fig. 11) by changing color. The addition of Hg^{2+} to an acetonitrile solution of **24** resulted in a color change to vermeil from yellow due to complexation. Sensor **24** has an LOD of 9.22×10^{-9} M towards Hg^{2+} ions.

4-Amino-1,8-napthalimide based fluorogenic probe **25**[76] has been developed to detect Hg^{2+}, and it contains iminodiacetic acid and picolinic acid as receptors. Sensor **25** is highly selective and sensitive towards Hg^{2+} in HEPES buffer solution (pH = 7.4) with a moderate LOD of 1.03×10^{-7} M. A reduced PET process due to the binding of Hg^{2+} with the picolinic acid and iminodiacetic acid receptor of **25** (Fig. 11) is responsible for the turn-on fluorescence signal. Due to the turn-on fluorescence feature, **25** is also able to image cells in the presence of Hg^{2+}.

Colorimetric fluorescent sensors have their own advantages due to their dual-mode of signaling, *i.e.*; by the naked eye and under UV light. Sensor **26**,[77] which is based on one indole ring (Fig. 12), is a typical example of a colorimetric fluorescent probe. Sensor **26** was applied for the detection of Hg^{2+} in HEPES buffer solution (pH = 7.0) by changing the color of the system from light yellow to pink and quenching the emission with a detection limit of 1.08×10^{-6} M. 1 : 1 binding between Hg^{2+} and **26** resulted in a color change and fluorescence quenching. Sensor **26** can successfully image HeLa cells at pH 7.4 in the presence of Hg^{2+}.

An imidazo[1,2-*a*]pyridine-based fluorogenic probe **27**[78] was developed to detect Hg^{2+}. Sensor **27** (Fig. 12) was able to detect Hg^{2+} in a fluorescence turn-off fashion in EtOH–water (8 : 2, v/v) medium. A 2 : 1 binding stoichiometry is observed between **27** and Hg^{2+} with an excellent detection limit of 1 ppb with imaging of HeLa cells. Unfortunately, **27** suffers from interference by Fe^{3+}.

Earlier we discussed one ESIPT sensor. Another ESIPT sensor **28**[79] is a Schiff base type system where an 8-aminoquinoline moiety acts as the binding site for Hg^{2+} ions (Fig. 12). In MeCN–water (3 : 2, v/v, 10 mM HEPES buffer, pH = 7.0) medium, sensor **28** is able to sense Hg^{2+} with a detection limit of 0.11 μM. Upon binding of Hg^{2+} with **28**, a strong emission signal is observed due to the disruption of the ESIPT process. Sensor **28** is useful for detecting Hg^{2+} at the cellular level due to the intense emission signal. Again, an ESIPT probe **29**[80] was also developed for the detection of Hg^{2+}. Sensor **29** (Fig. 13) differentiates Hg^{2+} from other competitive ions in a fluorescence turn-on fashion in DMF–HEPES solution (1 : 1, v/v, 10 mM, pH = 7.4). The free probe shows a very weak emission as it is in both PET and ESIPT active mode. Upon the addition of mercury, both processes are disrupted to turn on the intense emission. This change in emission from off to on demonstrates the sensing ability of **29** with an LOD of 6.45×10^{-6} M.

Similar to PET, ESIPT, AIEE, *etc.*, TICT is also a well-known phenomenon in the case of fluorescence spectroscopy. Sensor **30**[81] is an example of a TICT-active probe, where naphthalene diimide acts as the signaling unit. It can detect Hg^{2+} in acetone medium with a change in emission from colorless to red with a moderate LOD of 3 μM. The change in emission is attributed to the restriction of the TICT process of **30** due to binding with Hg^{2+}. Another TICT-active molecule **31**[82] was developed with naphthalene diimide as a signaling unit and bis[2-(3,5-dimethylpyrazole-1-yl)ethyl]amine as an electron donor and ligand for the binding of Hg^{2+}. In an acetone–water (1 : 1) medium, sensor **31** can recognize Hg^{2+} (Fig. 14) with a change in fluorescence from colorless to red. The sensing mechanism is quite similar to that of sensor **30**. With a 1.3×10^{-6} M detection limit, sensor **31** is useful for carrying out a biological study for the detection of Hg^{2+} in MCF-7 cells.

Benzothiazole-based sensor **32**[83] is an example of a colorimetric and fluorescent probe. The addition of Hg^{2+} to **32** (Fig. 15) in CH_3CN–water (1 : 1, v/v, pH = 8.0) medium resulted in a change in color from pink to blue accompanied by a strong emission signal at 425 nm. Thus **32** can be applied to detect Hg^{2+} with a significant range of 2.5 μM by UV-vis and 1.8 ppb by fluorescence emission.

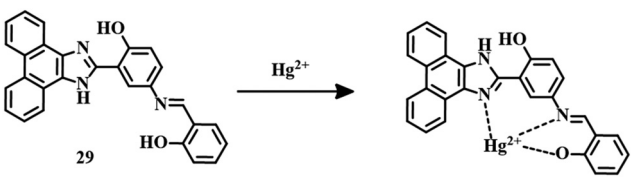

Fig. 13 The chemical structure and proposed sensing mechanism of **29**.

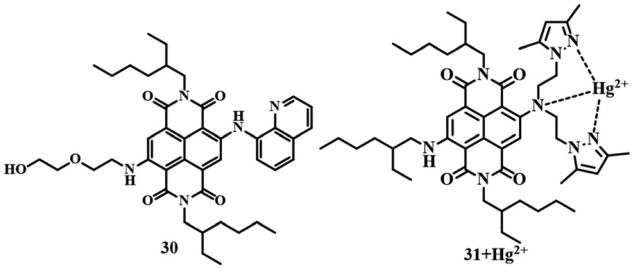

Fig. 14 The chemical structures of **30** and **31**–Hg^{2+}.

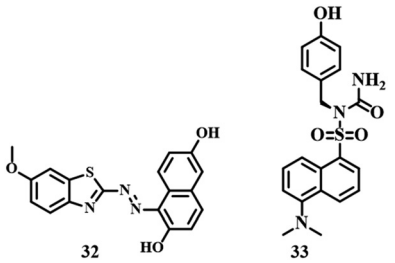

Fig. 15 The chemical structures of **32** and **33**.

A combination of dansyl group and tyrosine developed a turn-on fluorescence sensor **33**[84] which was applied to detect Hg^{2+} in HEPES buffer solution (pH = 7.4). With interaction between two molecules of the sensor **33** (Fig. 15) and one Hg^{2+}, the distance between dansyl units is reduced forming a dimer which is responsible for the enhanced fluorescence signal. Such high selectivity and an impressive LOD of 22.65×10^{-9} M towards Hg^{2+} make sensor **33** an excellent detection system with cell imaging capability.

We have discussed chemosensors which are based on ligand systems attached to some signaling units. Systems based on different phenomena such as ICT, PET, ESIPT, TICT, and AIEE have been used for the detection of Hg^{2+} by UV-vis and fluorescence spectroscopic techniques. Not all them but many of these sensors can image the cell in the presence of mercury. A summary of the information about the above-mentioned sensors is given in Table 1.

2.2 Rhodamine-based ligand systems for the detection of Hg^{2+}

We have discussed heteroatom-based ligand systems (**1–33**) which consist of different fluorogenic and chromogenic moieties apart from rhodamine, for the detection of Hg^{2+}. Among several dyes available as a fluorophore, rhodamine dyes are well known for their unique features, such as high absorption coefficient, long excitation wavelength, strong absorption, emission signal in the visible range and high quantum yield. Due to such extensive features, rhodamine is being used as the basic unit for the development of fluorescent and colorimetric probed to detect metal ions.[85–89] In this section we are going to discuss reported Hg^{2+} sensors based on rhodamine derivatives with ligand systems.

For the binding of Hg^{2+}, a phthalaldehydic has been combined with rhodamine 6G to synthesize sensor **34**.[90] Spirolactam ring-closed derivative **34** formed a colorless solution in a MeOH–water (1 : 1, v/v) mixture with no emission. Upon the addition of Hg^{2+}, the solution instantly changed color to pink with a strong yellow fluorescence. Strong 1 : 1 binding between **34** and Hg^{2+} resulted in the spirolactam ring-opening of the rhodamine derivative (Fig. 16), credited with the color and fluorescence change with an excellent lower detection limit of 5 pM, Due to this turn-on

Table 1 A comparison of different chemo-sensors (**1–33**)

Compound	Medium	LOD	Type of sensing	Biological study
1	CH_3CN–water (1 : 1, v/v)	1.81×10^{-7} M	Turn-on fluorescence	NA
2	CH_3CN–HEPES (7 : 3, v/v)	36×10^{-9} M	Turn-on fluorescence	NA
3	DMF–water (2 : 3, v/v)	0.061×10^{-6} M	Ratiometric fluorescence	Done
4	DMSO–water (1 : 99, v/v)	14.7×10^{-9} M	Turn-on fluorescence	NA
5	Ethanol–water (3 : 7, v/v)	45.4×10^{-9} M	Turn-on fluorescence	NA
6	MeCN–water (1 : 1, v/v)	1.21×10^{-6} M	Colorimetric	NA
7	MeCN–H_2O (1 : 1, v/v)	32.8 ppb	Colorimetric	NA
8	DMSO–Tris–HCl (8 : 2, v/v)	3.11×10^{-8} M	Turn-off fluorescence	NA
9	MeCN–H_2O (3 : 7, v/v)	5.01×10^{-8} M	Turn-off fluorescence and colorimetric	NA
10	EtOH–water (6 : 4, v/v)	17.8×10^{-9} M	Turn-off fluorescence	Done
11	Buffered solution containing 1% DMSO	65×10^{-9} M	Turn-off fluorescence	Done
12	CH_3CN–water (5 : 95, v/v)	99 ppm	Colorimetric and turn-on fluorescence	NA
13	MeOH–HEPES (7 : 3, v/v)	5.7×10^{-9} M	Turn-on ratiometric fluorescence and colorimetric	Done
14	DMSO–water (1 : 99, v/v)	591.9×10^{-9} M	Turn-on fluorescence	NA
15	CH_3CN	7.46×10^{-6} M	Turn-off fluorescence	Done
16	MeOH–water (1 : 4, v/v)	3.12×10^{-9} M	Turn-off fluorescence	Done
17	MeOH–Tris–HCl (5 : 95, v/v)	7.38×10^{-9} M	Turn-off fluorescence and colorimetric	NA
18	Water	0.34×10^{-6} M	Colorimetric and turn-off fluorescence	NA
19	HEPES buffer	1.24 μM	Turn-on fluorescence	Done
20	CH_3CN–water (1 : 9, v/v)	1.24×10^{-6} M	Turn-off fluorescence	NA
21	Water	0.138 ppm	Turn-on ratiometric fluorescence	NA
22	CH_3CN–HEPES (6 : 4, v/v)	2.94×10^{-9} M	Turn-off fluorescence	NA
23	Methanol–water (1 : 1, v/v)	4.7×10^{-7} M	Colorimetric	NA
24	CH_3CN	9.22×10^{-9} M	Colorimetric	
25	HEPES buffer	1.03×10^{-7} M	Turn-on fluorescence	Done
26	HEPES buffer	1.08×10^{-6} M	Turn-off fluorescence and colorimetric	Done
27	EtOH–water (2 : 8)	1 ppb	Turn-off fluorescence	Done
28	MeCN–water (3 : 2, v/v)	0.11×10^{-7} M	Turn-on fluorescence	Done
29	DMF–HEPES solution (1 : 1, v/v)	6.45×10^{-6} M	Turn-on fluorescence	Done
30	Acetone	3×10^{-6} M	Turn-on	NA
31	Acetone–water (1 : 1, v/v)	1.3×10^{-6} M	Turn-on	Done
32	CH_3CN–water (1 : 1, v/v)	2.5×10^{-6} M	Colorimetric and turn-on fluorescence	NA
33	HEPES buffer	22.65×10^{-9} M	Turn-on fluorescence	Done

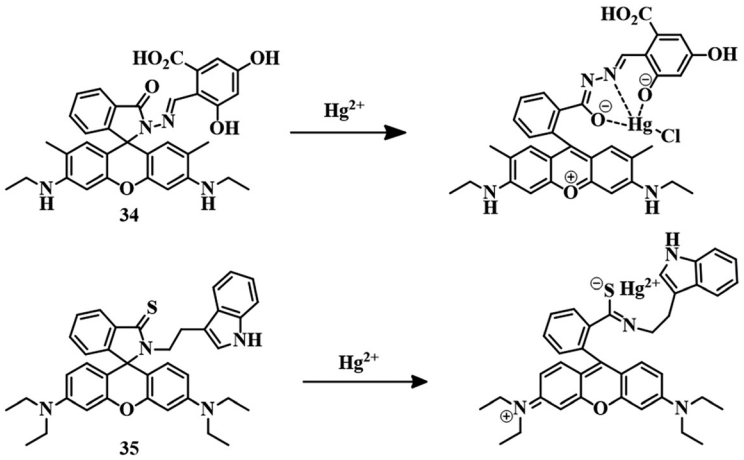

Fig. 16 The chemical structures of sensors **34** and **35** along with their proposed sensing mechanism.

fluorescence behavior of **34**, it has been used for the detection of Hg^{2+} in HeLa and macrophage cells.

Sensor **35**[91] is a rhodamine–tryptamine-coupled fluorogenic and chromogenic sensor. Tryptamine is analogous to tryptophan and acts as a neurotransmitter. The carbonyl oxygen of rhodamine is replaced by sulfur as Hg^{2+} has a high affinity towards thio groups. Initially, **35** has no color or fluorescence in MeOH–water (7 : 3) medium, but the sudden appearance of a pink color along with orange-red emission has been observed upon the addition of Hg^{2+}. The high thiophilic affinity of Hg^{2+} results in spirolactam ring-opening (Fig. 16) and a simultaneous change in color and fluorescence. A strong 1 : 1 binding stoichiometry between Hg^{2+} and **35** and naked-eye visualization of a change in color as well as fluorescence established the excellent sensing capacity of the sensor with an extremely low detection limit of 2.1 nM.

Another rhodamine-derived sensor **36** has been applied for the detection of Hg^{2+}. Slight modification has been undertaken to make the sensor different from the rhodamine B unit, where one side of the xanthene moiety has been substituted by piperazine and further functionalized with naphthyl chloride to develop sensor **36**.[92] A closed spirolactam ring has been formed by the introduction of hydrazine, which acts as the binding segment for Hg^{2+}. In an MeCN–water (7 : 3, v/v) mixture, sensor **36** showed no color or emission. But upon the introduction of Hg^{2+} to the solution, the sudden appearance of a pink color and yellow fluorescence has been observed. Initial binding of Hg^{2+} (Fig. 17) with **36** induces spirolactam ring-opening followed by hydrolysis for the formation of rhodamine acid, leading to the change in color as well as fluorescence. Sensor **36** has a moderate LOD of 0.38 μM and can be applied to stain living cells. Similarly, a combination of thioxorhodamine B hydrazine with [2,2′-bithiophene]-5-carboxaldehyde and [2,2′-bithiophene]-5,5′-dicarboxaldehyde leads to the development of sensors **37a** and **37b**, respectively.[93] These two sensors have different modes of action, although Hg^{2+}–induced spirolactam ring-opening is common to both. The sensing behavior of both sensors was carried out in EtOH–HEPES (1 : 1) medium. Initially, the solutions of both **37a** and **37b** have no color or emission. Upon the addition of Hg^{2+}, both showed a pink color with reddish-orange emission. Complexation of Hg^{2+} with **37a** triggers spirolactam ring-opening to activate the color and fluorescence of the rhodamine unit upon the excitation wavelength of the bithiophene moiety which suggests a FRET mechanism. In the case of **37b**, the sensing mode is different from that of **37a**, a traditional Hg^{2+}–induced spirolactam ring-opening upon binding in the cavity formed by thiophene and rhodamine unit is credited with the color change and emission change. The LOD values for **37a** and **37b** are 3.1×10^{-9} M and 2.92×10^{-9} M, respectively. These naked-eye fluorescent sensors are capable of detecting Hg^{2+} in living cells. The proposed sensing mechanisms of **37a** and **37b** are mentioned in Fig. 18.

Another sensor **38**[94] was designed by the attachment of hexaphenylbenzene and rhodamine units (Fig. 19). Initially, sensor **38** showed AIEE in a water–MeCN (1 : 1) mixture and formed fluorescent aggregates. The aggregates showed blue fluorescence due to the stacking of hexaphenylbenzene units. After the addition of Hg^{2+} to the solution, the fluorescence signal of 475 nm (blue emission) decreased and a new signal at 582 nm (orange-red emission) appeared with an intense pink color. The opening of the

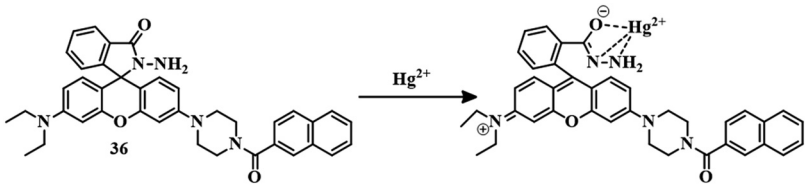

Fig. 17 The chemical structure and proposed sensing mechanism of sensor **36**.

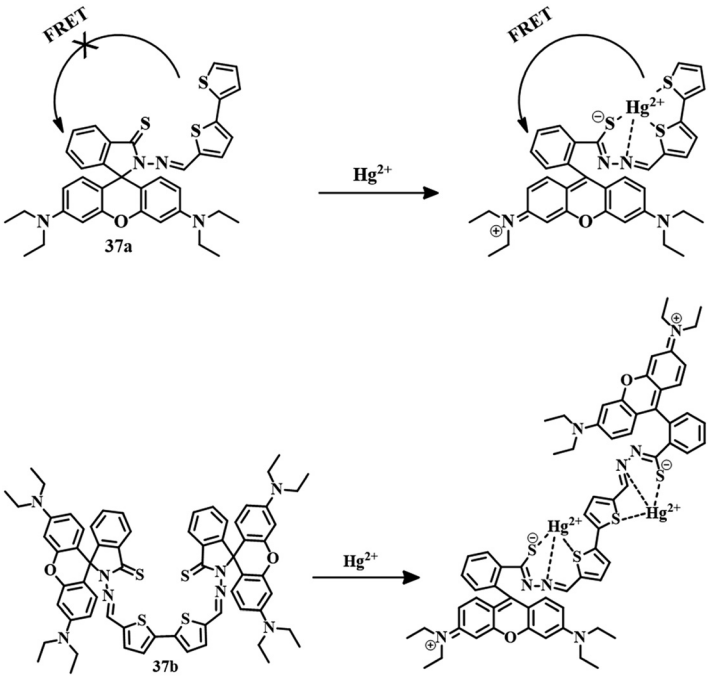

Fig. 18 The chemical structures of **37a** and **37b** and their proposed sensing mechanisms.

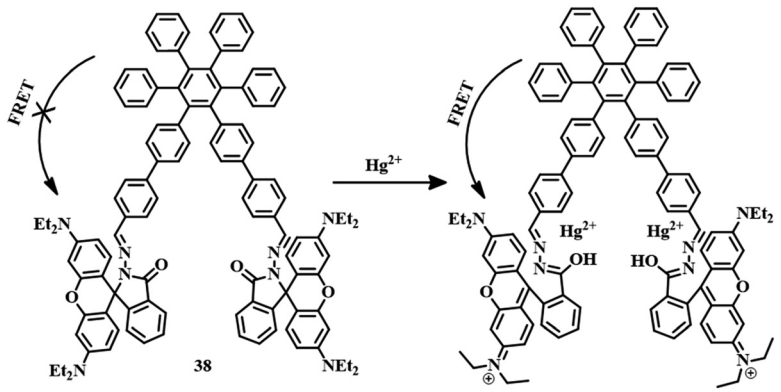

Fig. 19 The chemical structure and proposed sensing mechanism of **38**.

spirolactam ring by Hg^{2+} triggers the FRET process from hexaphenylbenzene (donor) to the rhodamine unit (acceptor). Thus, sensor **38** has evolved as an excellent tool for the detection of Hg^{2+} both in water sources and at a cellular level with a detection limit of 100 nM.

Slightly modified rhodamine B derivative **39**[95] was developed by the reaction between thiocarbonyl-functionalized rhodamine B and different substituted cinnamyl aldehydes. In an EtOH–water (1 : 1, v/v, PBS, Ph 7.4) mixture, all the derivatives of **39** have been applied for the detection of Hg^{2+} with the same mode of action. Spirolactam ring-opening and binding of Hg^{2+} through C═S and C═N segments resulted in a color change and fluorescence change (Fig. 20). All the derivatives are capable of tracking Hg^{2+} in living cells as well as in animal systems. The sensor consisting of H-functionalized cinnamyl aldehyde, has the maximum efficiency towards Hg^{2+} detection.

Another sensor **40**,[96] a combination of diphenyl selenium and rhodamine B hydrazide was applied for the selective and sensitive detection of Hg^{2+} in MeOH–water (9 : 1, v/v) medium. Traditional Hg^{2+}-induced spirolactam ring-opening followed by complexation with **40** resulted in a color change and fluorescence change (Fig. 20). With an impressive LOD of 12 nM, sensor **40** is capable of detecting Hg^{2+} in living cells and zebrafish. A similar kind of rhodamine 6G derivative **41**[97] has been developed for the selective and sensitive detection of Hg^{2+} in DMSO–water (1 : 1) medium with an acceptable LOD of 2.07×10^{-8} M. An initial weak emission band at 575 nm of **41** is due to a PET process but after the addition of Hg^{2+}, a drastic enhancement in fluorescence intensity at 575 nm has been observed as a result of a chelation-enhanced fluorescence (CHEF) process (Fig. 20). The visual detection ability of

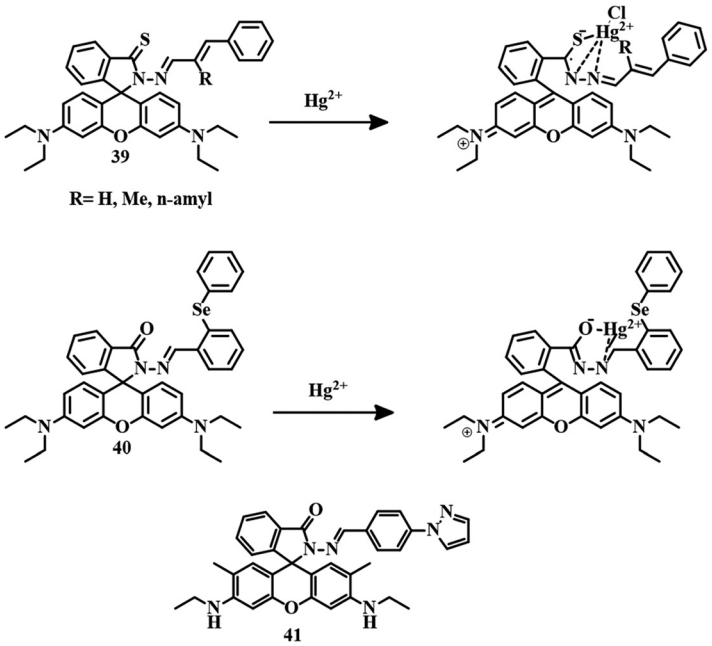

Fig. 20 The chemical structures of **39**, **40**, and **41**, and the proposed sensing mechanisms of **39** and **40**.

41 enabled the development of paper strips for the detection of Hg^{2+}.

From the condensation of thiobisethylamine with rhodamine B was developed a simply synthesized sensor **42**.[98] A solution of **42** in MeCN–HEPES (1 : 99, v/v) showed no color and no fluorescence, but the addition of Hg^{2+} resulted in a sudden color change and fluorescence change. Complexation between Hg^{2+} and **42** through an oxygen atom of the amide carbonyl group, S, and N atoms of the thiobisethylamine unit (Fig. 21) simultaneously opened the spirolactam ring which triggered the color and fluorescence change. With a moderate LOD of 0.14 μM, **42** has the capability of imaging cells in the presence of Hg^{2+}.

Another sensor **43**,[99] a combination of 2-hydroxy acetophenone and rhodamine hydrazine, was applied for the selective and sensitive detection of Hg^{2+} in an EtOH–water (2 : 1, v/v) buffer (10 mM, HEPES, pH = 7.2) mixture. The solution of **43** turned pink upon the addition of Cu^{2+} and Hg^{2+}, though enhanced reddish-orange fluorescence has been observed only in the case of Hg^{2+}. Strong 1 : 1 binding (Fig. 21) between the ion and **43** is attributed to spirolactam ring-opening and subsequent color and fluorescence change with a detection limit of 150 nM.

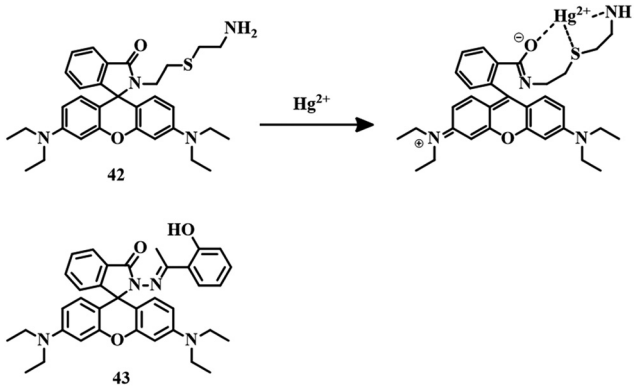

Fig. 21 The chemical structures of **42** and **43**. The proposed sensing mechanism of **42**.

A combination of a dialdehyde derivative of bisphenol A and N-(rhodamine-B) lactam-ethylenediamine developed a dual-channel probe **44**,[100] which has been applied for the selective detection of Hg^{2+} by the FRET phenomenon. In an MeCN–water (8 : 2, v/v, HEPES, Ph = 7.0) mixture, **44** showed an excellent pink color along with orange fluorescence upon the addition of Hg^{2+}. Spirolactam ring-opening of the rhodamine unit by Hg^{2+} forms a new conjugate system and activates the FRET process from the bisphenol (donor) unit to the rhodamine (acceptor) unit to give the orange emission as an output signal (Fig. 22). This emissive property of **44** can be used in the detection of Hg^{2+} in living cells.

Ratiometric sensor **45**,[101] a combination of a BODIPY unit and a rhodamine unit, was developed very cleverly. A combination of these two units has been used as a FRET pair, where the BODIPY unit can act as a donor and the rhodamine unit as an acceptor. These two units have been attached by a thiophene unit, which can act as a binding unit of Hg^{2+}. An ethanolic solution of **45** showed only a green fluorescence due to the BODIPY unit. But upon the addition of Hg^{2+}, reddish-orange emission observed upon excitation at 480 nm (BODIPY moiety) due to spirolactam ring-opening followed by FRET activation (Fig. 22). This FRET pair has an excellent LOD value of 1.56 ppb.

Sensor **46**[102] was also developed by the sequential reactions between rhodamine B, triethylenetetramine, and phenyl isothiocyanate (Fig. 23). Thiourea segments of **46** are responsible for the interaction with Hg^{2+}. In MeCN–HEPES (9 : 1, v/v) medium, **46** and Hg^{2+} formed a stable 1 : 3 complex with a strong orange emission accompanied by a pink color. Similarly, another rhodamine-based sensor **47** (Fig. 23) has been

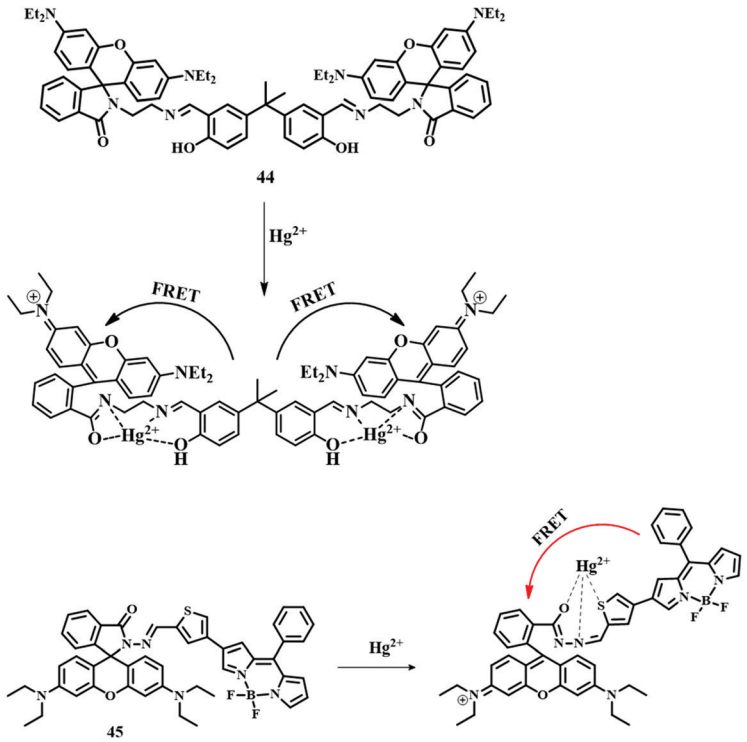

Fig. 22 The chemical structures of **44** and **45** and their proposed sensing mechanisms.

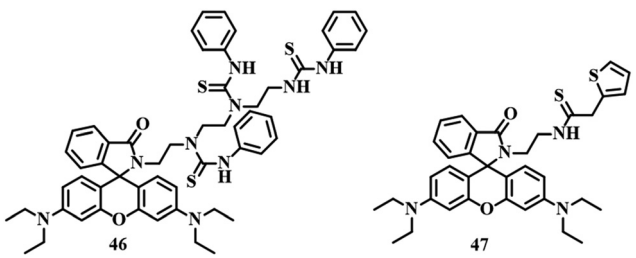

Fig. 23 The chemical structures of **46** and **47**.

developed with the combination of rhodamine B and -thiophene acetyl chloride.[103] This thiophene-coupled rhodamine derivative **47** was applied for the detection of Hg^{2+} in an EtOH–water (2 : 1, v/v) mixture. Spirolactam ring-opening induced by Hg^{2+}, followed by the complexation with **47** resulted in a pink coloration and reddish emission. An LOD of 0.11 μM and the ability to image living cells and zebrafish helped **47** to become a potential tool for the detection of Hg^{2+}.

In this section, we have discussed reported sensors of Hg^{2+} based on heteroatom-containing ligands and rhodamine units as the signaling moiety. The rhodamine unit has been successfully used as the signaling unit as it has both colorimetric and fluorometric properties in spirolactam ring-closed form. Rhodamine-based sensors can show turn-off to turn-on fluorescence activity upon interaction with metal ions. Hg^{2+} can induce the opening of the spirolactam ring in rhodamine derivatives and switch on the color as well an emission. Due to this unique feature, modified rhodamine molecules are one of the most commonly used tools for the detection of Hg^{2+} ions. All the comparative data are described in tabular form in Table 2.

2.3 Reaction-based irreversible sensors for Hg^{2+}

The above-mentioned sensor systems can detect Hg^{2+} complexation with the ligands and they can also be reversible. These interaction-based systems are one kind of developed tool that can be used for the detection of analytes, but there is always a chance of interference by other metal ions with the same type of chemical properties. But reaction-based detection systems are preferable due to their high selectivity over other competitive metal ions. Thioacetal deprotection, 1,3,4-oxadiazole formation, ester hydrolysis, hydrolysis of an imine bond, and alkyne or vinyl ether oxymercuration are well-known reactions which are preferably carried out by Hg^{2+}. These reactions have been used to design and develop different sensing systems for Hg^{2+} over the years. In this section, we are going to discuss reaction-based sensing systems that have evolved over the last few years.

2.3.1 Thioacetal deprotection. Thioacetal deprotection is one of the most important reactions which is done selectively by the Hg^{2+} ion. Using this to their advantage, many sensing systems have been developed to sense mercury with high selectivity. With this virtue, a simple benzothiazole-based fluorescent probe **48**[104] has been designed for the detection of Hg^{2+}. In this compound, one of the aldehyde groups has been protected by 1,3-propanedithiol to form thioacetal which is the reaction site for Hg^{2+}. Initial green fluorescence of **48** in PBS buffer (pH 7.4, containing 2% DMSO) solution is observed

Table 2 A comparison of different rhodamine-based chemosensors (**34–47**) for Hg^{2+}

Compound	Medium	LOD	Type of sensing	Biological study
34	MeOH–water (1 : 1, v/v)	5×10^{-12} M	Colorimetric and turn-on fluorescence	Done
35	MeOH–water (7 : 3, v/v)	2.1×10^{-9} M	Colorimetric and turn-on fluorescence	NA
36	MeCN–water (7 : 3, v/v)	0.36×10^{-6} M	Colorimetric and turn-on fluorescence	Done
37a	EtOH–HEPES (1 : 1, v/v)	3.1×10^{-9} M	Colorimetric and turn-on fluorescence	Done
37b	EtOH–HEPES (1 : 1, v/v)	2.92×10^{-9} M	Colorimetric and turn-on fluorescence	Done
38	MeCN–water (1 : 1, v/v)	100×10^{-9} M	Colorimetric and turn-on fluorescence	NA
39	EtOH–water (1 : 1, v/v, PBS, pH = 7.4)	8.26×10^{-9} M, 15.52×10^{-9} M, 23.26×10^{-9} M	Colorimetric and turn-on fluorescence	Done
40	MeOH–water (9 : 1, v/v)	12×10^{-9} M	Colorimetric and turn-on fluorescence	Done
41	DMSO–water (1 : 1, v/v)	2.07×10^{-8} M	Colorimetric and turn-on fluorescence	NA
42	MeCN–HEPES (1 : 99, v/v)	0.14×10^{-6} M	Colorimetric and turn-on fluorescence	Done
43	EtOH–water (2 : 1, v/v)	150×10^{-9} M	Colorimetric and turn-on fluorescence	NA
44	MeCN–water (8 : 2, v/v, HEPES, Ph = 7.0)	2.16×10^{-6} M	Colorimetric and turn-on fluorescence	Done
45	EtOH	7.8×10^{-9} M	Colorimetric and turn-on fluorescence	NA
46	MeCN–HEPES (9 : 1, v/v)	3.04×10^{-7} M	Colorimetric and turn-on fluorescence	NA
47	EtOH–water (2 : 1, v/v)	0.11×10^{-6} M	Colorimetric and turn-on fluorescence	Done

due to the ESIPT process between the benzothiazole moiety and adjacent –OH group as well as due to the presence of the electron-donating group thioacetal. After the addition of Hg^{2+}, green fluorescence shifted to blue fluorescence in a ratiometric manner. Hg^{2+} deprotects the thioacetal to form an electron-withdrawing aldehyde group which is the reason for the observed blue shift in emission (Fig. 24). Due to this deprotection behavior of Hg^{2+} towards thioacetal groups, **48** becomes a highly selective and ratiometric fluorescent tool for sensing purposes with an LOD of 7.6×10^{-9} M. Sensor **48** also has the capability of sensing mercury ions in biological systems.

Similarly, an oligothiophene-based thioacetal system **49**[105] has been developed as an excellent colorimetric and fluorometric probe for the detection of Hg^{2+} in EtOH–water (1 : 1) medium. Sensor **49** has a strong blue fluorescence due to the stopped ICT process as well as having no color. But upon addition of Hg^{2+}, the color of **49** changed from colorless to yellow accompanied by yellow fluorescence. The formation of an aldehyde group from thioacetal is promoted by Hg^{2+} (Fig. 24) which activates the ICT process, which is responsible for the color change as well as the fluorescence change. Sensor **49** can detect Hg^{2+} in water, soil, and seafood with a detection limit of 1.03×10^{-8} M.

Benzothiazole-based "ESIPT + AIE"-active probe **50**[106] was designed for the selective detection of Hg^{2+} in THF–water (1 : 1, v/v, PBS, Ph = 8.5) medium. The aldehyde group was protected by 3-marceptopropionic acid to make it an Hg^{2+}-reactive compound. Hg^{2+}-triggered hydrolysis of **50** (Fig. 25) resulted in the formation of an "ESIPT-AIE"-active molecule which shows a strong yellow fluorescence. This distinct change in emission can be effectively applied for biological study. Sensor **50** has an impressive detection limit of 1.59×10^{-8} M. Similarly a colorimetric and fluorescent probe **51**,[107] based on a benzo[1,2-*b*:4,5-*b*′]dithiophene (BDT) unit has been developed for the detection of Hg^{2+}, where a thioacetal group is used as the reaction site. Sensor **51** has been applied for the detection of Hg^{2+} in a THF–water (1 : 1) mixture with a change of color to yellow from colorless and yellow emission from blue. Thioacetal deprotection to aldehyde formation (Fig. 25) of sensor **51** promoted by Hg^{2+} is the reason behind the color change as well as the emission change. Due to its reaction-based sensing mechanism, sensor **51** emerged as a highly selective Hg^{2+} sensor with a moderate LOD of 3.1×10^{-7} M.

A 1,3-dithiane group has been incorporated into a dicyanomethylene-4*H*-pyran fluorophore for the design of a dual colorimetric and NIR fluorescent probe **52**.[108] Sensor **52** has been applied for the detection of Hg^{2+} in a PBS–DMSO buffer (20 mM, pH 7.4, 5 : 5, v/v) mixture. Hg^{2+}–Induced deprotection of the thioacetal segment changes the color to pink from purple with an emission signal around the NIR area (Fig. 26). **52** can

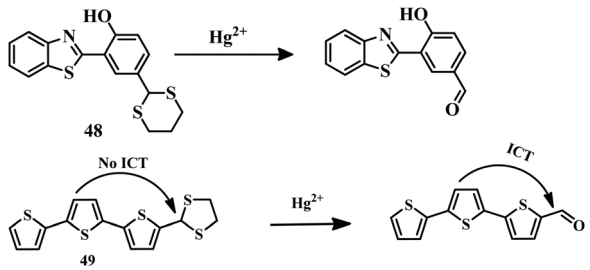

Fig. 24 The chemical structures and proposed sensing mechanisms of **48** and **49**.

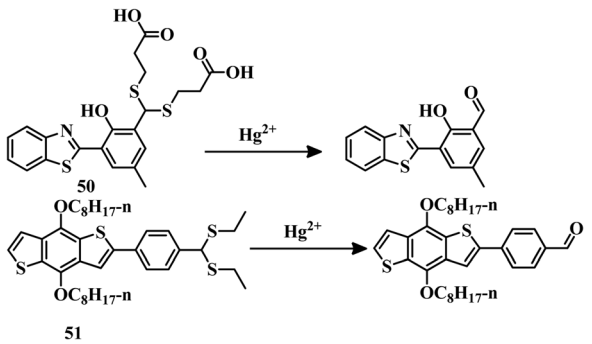

Fig. 25 The chemical structures and proposed sensing mechanisms of **50** and **51**.

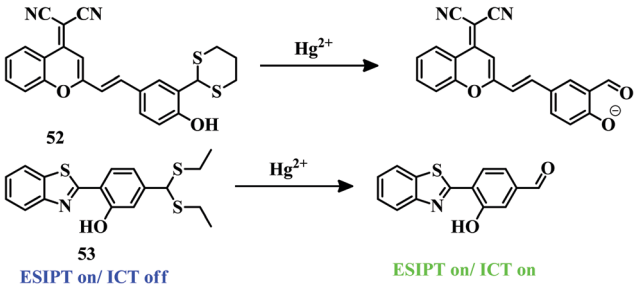

Fig. 26 The chemical structures and proposed sensing mechanisms of sensors **52** and **53**.

successfully detect selectively only Hg^{2+} among other metal ions due to the thiophilic nature of mercury. This dual-channel detection system has an LOD value of 6.8×10^{-8} M. Due to its prominent and visual color change as well as emission signal around the NIR zone, it can be applied in biological systems and the environment for the detection of Hg^{2+}.

Another sensor **53**[109] consists of benzothiazole as a core unit. The presence of the thioacetal group stops the ICT process and activates the ESIPT between –OH and the benzothiazole unit; as a result, blue fluorescence has been observed in a pH 7.4, 10 mM HEPES buffer–ethanol (1 : 1, v/v) mixture. Upon addition of Hg^{2+} to the mixture of **53**, intense greenish-yellow emission was observed by decreasing the blue emission. ICT along with ESIPT has been activated due to the appearance of the –CHO group by Hg^{2+}-triggered deprotection of thioacetal (Fig. 26). Due to the ratiometric nature of the detection and low LOD of 5.8 nM, sensor **53** can act as a good tool for the detection of Hg^{2+}, though it lacks biological application.

A simple pyrene derivative **54a**[110a] containing a bisethylsulfane moiety has been applied to sense Hg^{2+} in semi-aqueous medium and biological systems. Sensor **54** can detect Hg^{2+} selectively due to the presence of the bisethylsulfane segment. Hg^{2+} promotes the removal of bisethylsulfane to produce 1-pyrenecarboxaldehyde (Fig. 27) in MeCN–water (1 : 1, v/v) medium with the appearance of blue emission. Sensor **54a** has a detection limit of 57 nM and can successfully detect Hg^{2+} in living cells and zebrafish.

Another dithiolane-based probe **54b**[110b] has been successfully applied to identify Hg(II) in ethanol/water (2 : 8, v/v; pH = 7.40) medium. Due to the protected form of the –CHO group in the naphthalene moiety, the fluorescence intensity is weak initially. After addition of Hg(II), a colour change to light green from light yellow and strong emission were observed. This change in colour and emission is expected due to the transformation of dithiolane to a formyl group (Fig. 27). Sensor **54b** turned out to be an excellent sensor for Hg(II) with a detection limit of 4.0×10^{-8} M and ability for cell imaging.

Probe **54c**[110c] has been reported as an excellent small molecular probe for Hg(II) detection. In a 99% PBS buffer solution of **54c**, with the addition of Hg(II), the solution turned green-emissive from non-emissive. Here also the dithiolane segment has been used as selective reaction site for Hg(II). By virtue of this the formation of a –CHO group triggered by Hg(II)

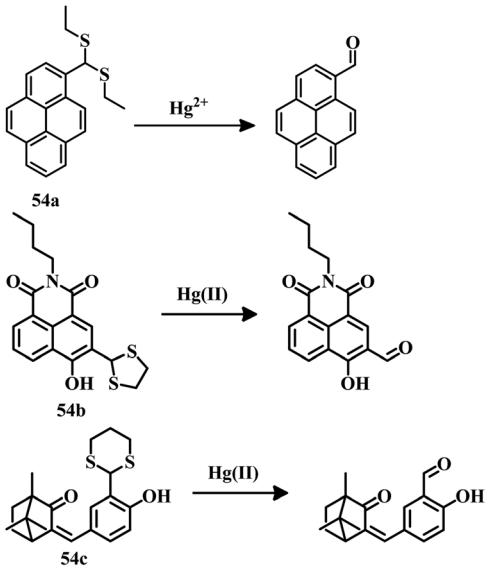

Fig. 27 The chemical structures and proposed sensing mechanisms of **54a**, **54b** and **54c**.

leads to the observed green emission (Fig. 27). As a reaction-based sensor, **54c** is highly selective towards Hg(II) and suffered zero interference by other analytes. It has been successfully applied in a paper-strip model and for analysis of Hg(II) contamination in real samples. The limit of detection for **54c** is calculated as 19.3 nM.

Another sensor **55** consists of a π-extended anthracene moiety bearing thioacetal segments within it.[111] In a solution of a THF–PBS buffer (1 : 1, v/v, pH = 7.4) mixture, sensor **55** showed weak blue fluorescence. After the addition of mercury, successful deprotection of thioacetal formed the aldehyde. Aldehyde formation from thioacetal (Fig. 28) triggered the intense green emission which contributed to the effectiveness of the chemodosimetric nature of **55** with an LOD of 59 nM. Due to this ratiometric change in emission, **55** was utilized for the detection of Hg^{2+} in living cells.

Coumarin-based fluorescent probe **56**[112] was developed by introducing a 2-aminophenyl group to the Hg^{2+}/CH_3Hg^+-reactive thioacetal group. In a PBS buffer solution of **56**, the introduction of Hg^{2+} ions resulted in aldehyde formation from thioacetal followed by condensation with an adjacent $–NH_2$ group to form a heterocyclic aromatic compound with large conjugation (Fig. 28). Due to the formation of the heterocyclic aromatic compound with a coumarin ring, bright green emission was observed with the shifting of the emission spectrum. Sensor **56** is able to detect both Hg^{2+} and CH_3Hg^+ with the same mode of sensing mechanism and green emission as an output signal. The LOD values are 27 nM and 5.7 μm for Hg^{2+} and CH_3Hg^+, respectively.

In this section, we have discussed thioacetal-based probes for the irreversible detection of Hg^{2+} in the environment and biological systems.

2.3.2 Vinyl ether oxymercuration. The hydrolysis of vinyl ether by Hg^{2+} is one design that can make the sensor highly selective. This so-called oxymercuration reaction can overcome

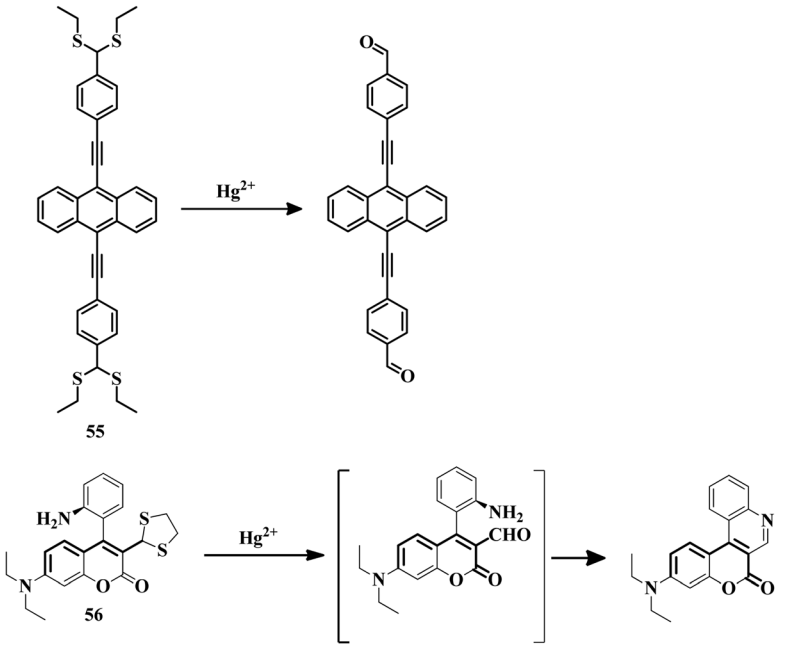

Fig. 28 The chemical structures and proposed sensing mechanisms of **55** and **56**.

the selectivity issue compared to probes based on heteroatom-containing ligands. Also, in most cases this vinyl ether hydrolysis leads to turn-on fluorescence which is much preferable for tracing Hg^{2+} as well as CH_3Hg^+ in both the environment and biological systems. In this section, we are going to discuss some reported chemodosimeters for mercury detection based on the hydrolysis of the vinyl ether group.

Fluorescent probe **57**[113] consisting of coumarin as a fluorophore moiety and vinyl ether as the reactive site was developed for the detection of Hg^{2+}. Sensor **57** in HEPES buffer solution showed no emission but upon addition of Hg^{2+} the sudden appearance of blue emission was observed. The irreversible hydrolysis reaction of the vinyl ether group promoted by Hg^{2+} (Fig. 29) is the reason behind the turn-on fluorescence response of **57** with a detection limit of 0.12 μM. Similarly, another sensor **58**[114] comprises an O–vinyl protected hydroxyl benzaldehyde coupled with rhodamine hydrazone. Initially **58** in CH_3CN–PBS buffer (3/7, v/v, 10.0 mM, pH = 7.40) solution exhibited green fluorescence due to the ICT process. After the addition of Hg^{2+}, the green fluorescence of **58** decreased due to the deprotection of the vinyl ether group which inhibited the ICT process (Fig. 29). With the turn-off emission of **58** in the presence of Hg^{2+}, it has a detection limit of 244 ppb.

Sensor **59**,[115] based on a vinyl ether derivative of hemicyanine, has been developed for the detection of Hg^{2+}. Deprotection of the –OH group of hemicyanine by a vinyl group blocks the ICT process. Hydrolysis of vinyl ether promoted by Hg^{2+} in **59** (Fig. 30) activates the ICT process in the HEPES buffer solution, which is responsible for the appearance of an orange color as well as reddish-yellow fluorescence. This drastic change in color and fluorescence of **59** appears to be advantageous in the field of Hg^{2+} detection with biological applications.

An NIR-fluorescent probe **60**[116] was developed, where 9-(2-carboxyphenyl)-6-(diethylamino)-1,2,3,4-tetrahydroxanthylium was used as a fluorophore and vinyl ether acted as the reactive site for Hg^{2+}. Sensor **60** in ethanol–H_2O (2 : 8, v/v 50 mM HEPES buffer solution, pH = 7.4) solution initially showed a weak red emission at 660 nm but upon the introduction of Hg^{2+}, a drastic enhancement in 660 nm peak with strong red emission was observed. This change in emission was due to the removal of the vinyl ether group and the formation of an –OH group which increases the ''push–pull'' property to activate the ICT process

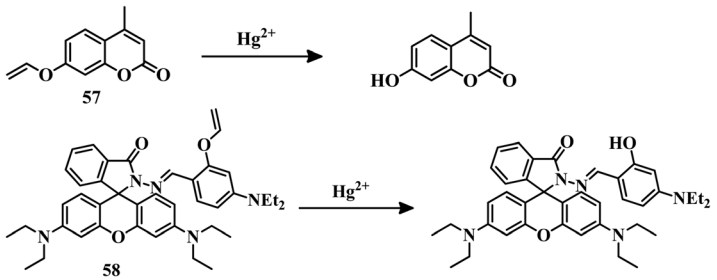

Fig. 29 The chemical structures of **57** and **58** along with their proposed sensing mechanisms.

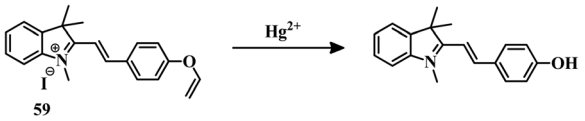

Fig. 30 The chemical structure and proposed sensing mechanism of **59**.

(Fig. 31). Due to the turn-off to turn-on nature of **60** in the presence of Hg^{2+}, it is very useful in the environment and biological systems. This NIR probe has an LOD value of 3.2 nM.

Another sensor **61**[117] was developed for the selective and sensitive detection of Hg^{2+} with the help of a vinyl ether group as the reaction site. Initially, blue fluorescence of **61** was observed in 10 mM PBS buffer (1% CH_3CN) solution which was due to the stopped ESIPT process. But after the addition of Hg^{2+} to the PBS buffer solution, an equivolume of DCM was added and fluorescence was recorded, a drastic red shift of the emission spectrum was observed with a cyan emission. Deprotection of the vinyl ether group promoted by Hg^{2+} and formation of –OH group (Fig. 31) activate the ESIPT process which was the reason for cyan fluorescence. Sensor **61** is an excellent chemodosimeter due to its ratiometric nature and an impressive LOD of 7.8×10^{-9} M. It can also be applied in biological systems to detect Hg^{2+} with good efficiency.

2.3.3 Other reaction-based sensors. In this section, we are going to discuss other reaction-based approaches for the detection of Hg^{2+}, such as hydrolysis of esters or imine bonds, and 1,3,4-oxadiazole formation. Sensor **62**[118] consists of a 2-mercapto-benzyl ester group as the reaction site forester hydrolysis. 4-[2-(4-Hydroxyphenyl)-vinyl]-1-methyl-pyridinium[*e*]iodide was used as the signaling unit due to its high water solubility. In a 100% PBS buffer solution, sensor **62** shows no emission due to the ester moiety which inhibits the intramolecular charge transfer process. But upon addition of Hg^{2+} ion, it coordinates with the –SH and C=O groups of the 2-mercapto-benzyl segment to facilitate the hydrolysis reaction to form an –OH group of the fluorophore (Fig. 32). This hydrolysis reaction triggers activation of the ICT process to show a green-yellow emission signal. Sensor **62** acted as a turn-on chemodosimeter for the detection of Hg^{2+} with a detection limit of 6.5 nM. Another sensor **63**,[119] a Schiff base type of compound containing benzimidazole and coumarin units as fluorophores, was developed for the selective detection of Hg^{2+} in HEPES buffer/DMSO (v/v = 9 : 1, pH = 7.2) medium. Initial weak blue emission turned intense blue upon the addition of Hg^{2+} into the solution of **63**. This enhanced emission signal is expected to be due to the cleavage of the imine bond by Hg^{2+} and the formation of the coumarin part (Fig. 32). With a high sensitivity of 70 nM, **63** can be applied for the detection of Hg^{2+} in biological systems.

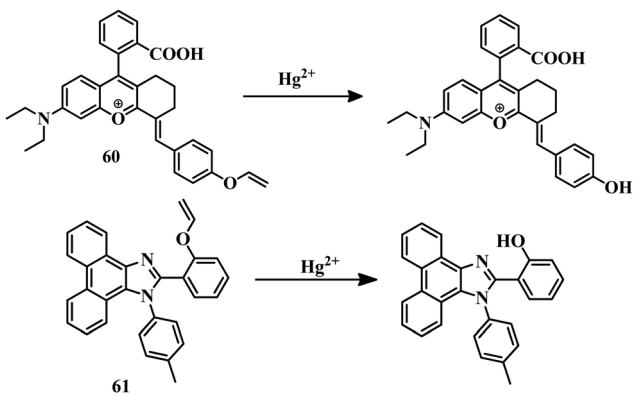

Fig. 31 The chemical structures and proposed sensing mechanisms of **60** and **61**.

Similarly, sensor **64**[120] was developed using a coumarin derivative and a 5-aminoisophthalic acid methyl ester unit. Due to the formation of the Schiff base between coumarin dye and the amino isophthalic acid methyl ester derivative in CH_3CN–H_2O (8/2, v/v, 0.1 M $KClO_4$ buffer, pH = 7.34) medium, no emission was observed. Upon the addition of Hg^{2+}, a highly intense peak at 490 was observed. The resulting emission signal corresponded to the coumarin aldehyde unit which was a result of imine bond cleavage promoted by Hg^{2+} to suppress the PET process (Fig. 33). Sensor **64** was successfully applied to detect mercury at the nanomolar level with biological applications.

An imidazo[1,2-*a*]pyridine-rhodamine ratiometric fluorescent probe **65**[121] was developed for the detection of Hg^{2+} in PBS/EtOH (9 : 1, v/v) medium. Upon addition of Hg^{2+} to the solution of **65**, it turned pink in color with a reddish emission. Hg^{2+} promoted spirolactam ring-opening followed by the formation of 1,3,4-oxadiazole by thiosemicarbazide (Fig. 34). Due to this new structure formation and extended conjugation, the FRET process was generated to give a unique color and emission. Sensor **65** has an LOD of 9.1 nM and the capability of tracking mercury at the cellular level with excellent efficiency.

Another sensor **66**[122] was developed as a pyrido[1,2-*a*]benzimidazole-rhodamine based FRET system. In this system, benzimidazole was used as the energy donor and a piperazine-functionalized rhodamine unit was used as the acceptor of energy. In a solution of EtOH–water (2 : 8, v/v), **66** shows blue emission with no color. After the addition of Hg^{2+}, the sudden appearance of a pink color with red emission was observed upon excitation at 380 nm which corresponds to the benzimidazole moiety. The mechanism is similar to that of sensor **65**, where the formation of 1,3,4-oxadiazole and spirolactam ring-opening (Fig. 34) is the reason behind the color change and emission change. Sensor **66** with a good LOD of 18.8 nM, can be applied for detecting Hg^{2+} in biological systems.

Sensor **67**[123] was developed with the combination of rhodamine B, *o*-phenylenediamine, and phenyl isothiocyanate. Initially a solution of **67** in MeCN–HEPES (1 : 9, v/v, pH = 7.2) medium showed no color and no emission. The addition of Hg^{2+} to the solution resulted in a pink color and reddish emission. Hg^{2+} promoted spirolactam ring-opening followed by the formation of a benzimidazole-appended rhodamine intermediate (Fig. 35) to generate the color as well as the emission output. The dual-mode of detection of **67** in a chemodosimetric manner made it much more useful with an LOD of 1.6 nM and biological applicability.

Another sensor **68** was designed with a perimidine moiety for the detection of Hg^{2+} ions. In a MeCN–water (3 : 7, v/v) mixture, **68a**[124a] showed no emission. A strong blue emission

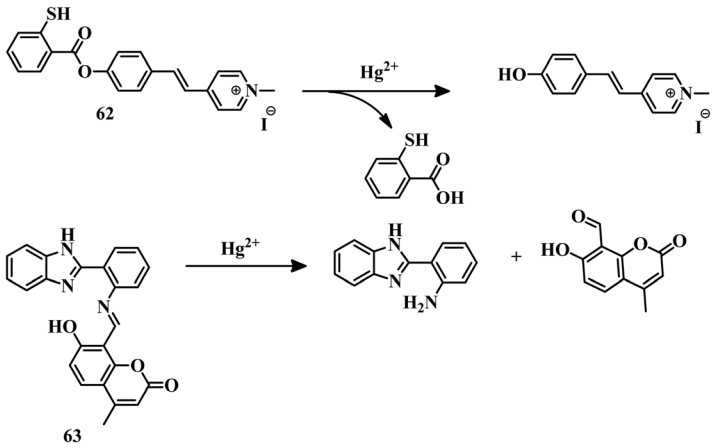

Fig. 32 The chemical structures and proposed sensing mechanisms of **62** and **63**.

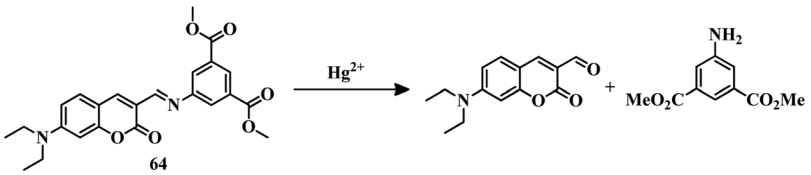

Fig. 33 The chemical structure and proposed sensing mechanism of **64**.

was observed for **68a** upon the addition of Hg^{2+}. The blue emission signal is attributed to the Hg^{2+}-mediated formation of a double bond in the junction of the coumarin and naphthalin moiety (Fig. 35). Sensor **68a** suffered from a low LOD of 1.08 μM although it can be applied in biological systems to detect Hg^{2+}.

Another azo-based sensor **68b**[124b] has been introduced for the successful colorimetric detection of Hg(II) in a DMSO–water (1 : 99, v/v) system. Here the Hg(II)-triggered desulfurization and subsequent rearrangement leads to the change in colour for **68b** (Fig. 35). This system is an excellent molecule to detect Hg(II) with an LOD of 8.1 nM and can be used as a solid chip to visualize the colour change.

A combination of the dye pyronin and the chelating agent *meso*-2,3-dimercaptosuccinic acid developed sensor **69**[125] for the detection and removal of Hg^{2+}. This one of the rare systems which can detect and sense Hg^{2+} ions. In PBS buffer solution, **69** remained in turn-off fluorescence mode and was colorless to the naked eye. Upon introduction of Hg^{2+}, a solution of **69** turned pink in color and emitted reddish fluorescence. Strong binding of Hg^{2+} with the ligand and subsequent removal of the chelated complex generated free pyronin dye to which was attributed the appearance of the pink color and reddish emission (Fig. 36). With the excellent dual-sensing signal and high LOD of 300 pM, sensor **69** was successfully applied at the cellular level and in a zebrafish model for tracking Hg^{2+}.

The thiocarbonate-appended fluorescein-based chemodosimeter **70**[126] was developed for the turn-on fluorescent detection of Hg^{2+} in a HEPES buffer solution (20 mM, pH 7.4, 1% EtOH). Initially, with no color and emission, **70** showed green emission upon the addition of Hg^{2+}. Hg^{2+} promotes the hydrolysis of the thiocarbonate segment and forms free fluorescein acid which results in a greenish emission (Fig. 36). Sensor **70** has a detection limit of 40 nM.

Another thiocarbonate-based sensor **71**[127] was developed, where 2-(2′-hydroxyphenyl)benzothiazole was used as the fluorophore unit. Benzothiazole segments are well known for their ESIPT activity as well as their AIEE activity. Upon functionalization of the –OH group, the ESIPT process stopped for **71**. An appearance of yellow fluorescence was observed in an EtOH–water (5/5, v/v, HEPES pH = 7.4) solution of **71** upon the addition of Hg^{2+} ions. This yellow color was generated due to the Hg^{2+}-triggered hydrolysis of thiocarbonate to form an –OH group and activate the ESIPT process (Fig. 37). Sensor **71** has a detection limit of 55 nM.

Similarly, sensor **72**[128] was designed based on the ESIPT phenomenon, where 2-(2′-hydroxyphenyl)benzothiazole also acted as a signaling unit and thiophosphate as a reaction site. Blocking of –OH group with thiophosphate deactivated the ESIPT process and turned off the emission. In a solution of CH_3CN/HEPES (1 : 4, v/v, 10 mM, pH = 7.4), **72** turned blue-emissive upon addition of Hg^{2+} ions. Removal of the thiophosphate group resulted in the formation of an –OH group (Fig. 37) which activated the ESIPT to give blue emission. With an LOD of 12 nM, **72** can be applied for the detection of Hg^{2+} at the cellular level.

In this section, we have successfully discussed Hg^{2+} sensors based on reactions, which are chemodosimetric in nature as they irreversibly detect the analyte. In comparison to heteroatom-containing ligand systems, reaction-based sensors are superior due to their excellent selectivity towards Hg^{2+} ions.

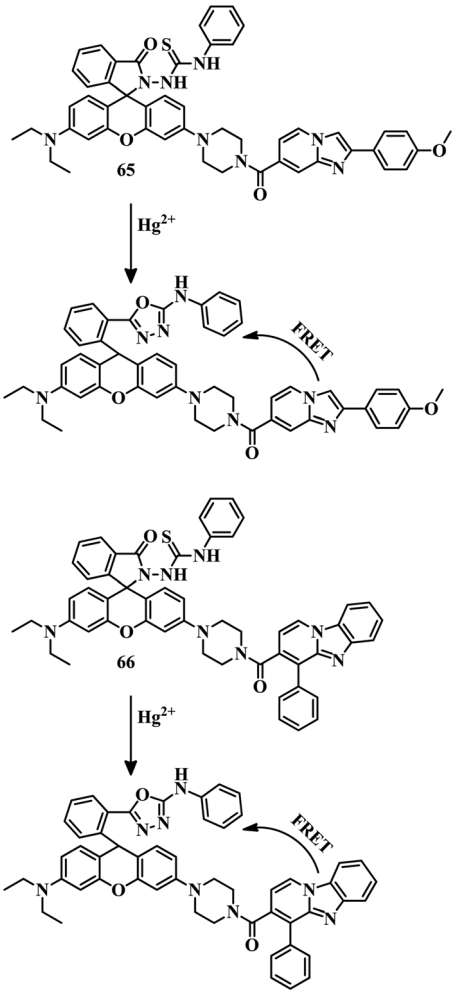

Fig. 34 The chemical structures and sensing mechanisms of **65** and **66**.

All the summarised information about reaction-based sensors (**48–72**), is given in Table 3.

2.4 Polymer-based sensors for the detection of Hg^{2+}

Above we have discussed small-molecule systems to detect Hg^{2+} ion in environmental sources and biological systems. Among the sensors (**1–72**), only a few compounds can detect Hg^{2+} in pure water or buffer medium. To overcome this issue, polymeric sensors were introduced for this detection process. Not only their water solubility but also the presence of many repeating units throughout the backbone, means polymers can produce highly amplified intensity to which can be attributed their high sensitivity.[129–134] Due to these advantageous features, polymeric materials have been developed in recent times for the detection of analytes such as Hg^{2+}. In this section, we are going to discuss some polymeric materials which were applied for the detection of Hg^{2+} ion under different conditions.

A dithioacetal-based conjugated polymeric sensor **73**[135] was developed for detecting Hg^{2+} in THF medium with high selectivity and sensitivity. Initial green fluorescence turned into red emission upon the addition of Hg^{2+} to a solution of **73**. The

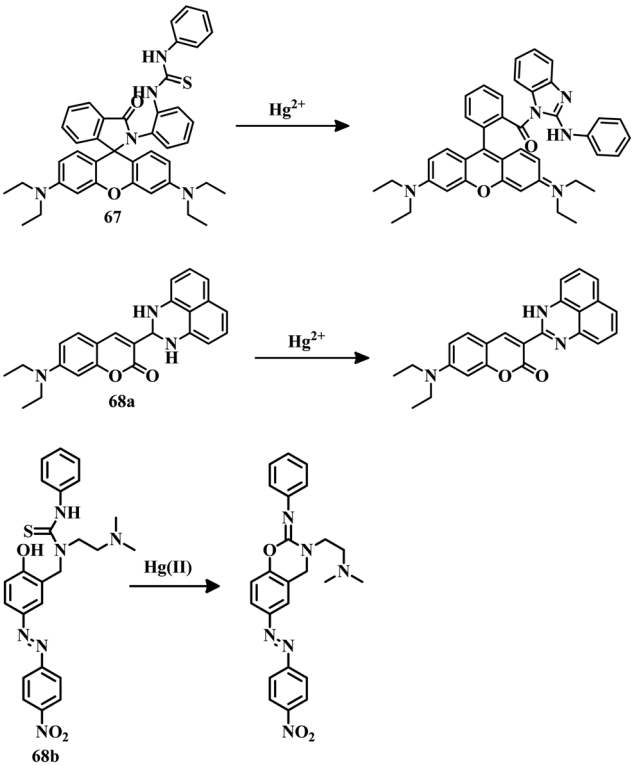

Fig. 35 The chemical structures and proposed sensing mechanisms of **67**, **68a** and **68b**.

intramolecular charge transfer process was inhibited in the dithioacetal containing **73**, but Hg^{2+} promoted deprotection of dithioacetal and the formation of –CHO group again triggered the ICT process to give red emission (Fig. 38). This visual color change of fluorescence for **73** can be used as a good tool for detecting Hg^{2+} with a detection limit of 1 μM.

Another polymeric sensor **74**,[136] consisting of a hydrophilic segment and a functionalized BODIPY segment, was developed for the detection of Hg^{2+}. A 4-amino phenol functionalized BDIPY unit used as the responsible site for Hg^{2+} sensing. Due to the water solubility of random polymer **74**, it can detect Hg^{2+} in a pure water medium. The appearance of a brown color and intense green emission was observed after the addition of Hg^{2+} to the solution of **74**. This drastic change in color and emission was due to the hydrolysis of the imine bond by Hg^{2+} and the formation of an aldehyde group (Fig. 38). Sensor **74** has an LOD of 1.10 μM.

Sensor **75**[137] is a thermoresponsive diblock copolymer with colorimetric detection ability towards Hg^{2+} ions. Polymeric sensor **75** has an LCST value of ~55 °C and is molecularly soluble in water. Below the LCST, PHPDEA units are exposed to water. Upon the addition of Hg^{2+}, the exposed PHPDEA unit is hydrolyzed to form the strong electron-withdrawing group cyanide. With this formation of a strong –CN group (Fig. 39), the intramolecular charge transfer process was maximized and an obvious sudden color change to pink from yellow was observed. But above LCST, **75** was unable to detect Hg^{2+} ions as the HPDEA units were then inside the hydrophobic core of the multi-molecular micelles. Sensor **75** was demonstrated as

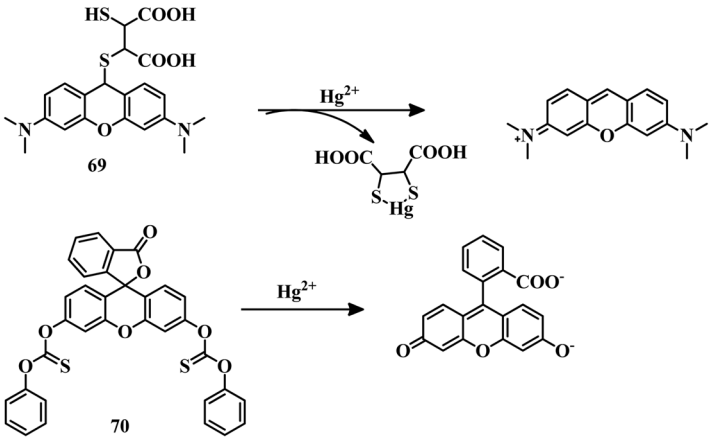

Fig. 36 The chemical structures and proposed sensing mechanisms of **69** and **70**.

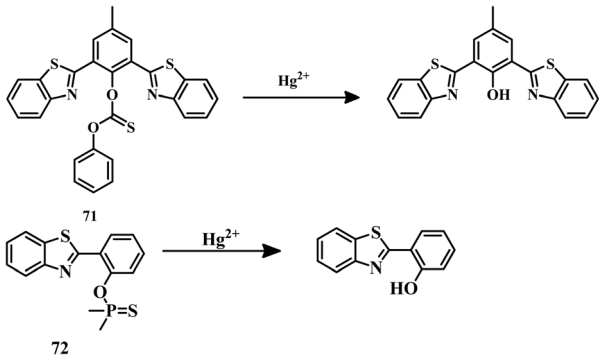

Fig. 37 The chemical structures and proposed sensing mechanisms of **71** and **72**.

an excellent highly selective tool for the detection Hg^{2+} colorimetrically with a detection limit of 0.03 mM.

Further stimuli-responsive polymeric sensors **76a** and **76b** were developed for the detection of Hg^{2+} in a colorimetric way with pH-tunable sensitivity.[138] Sensor **76a** was developed by the protection of the aldehyde group of the azo-polymer with ethanethiol and **76b** was developed by the protection of the aldehyde of the azo-polymer with 3-marcaptopropionic acid. These azo-polymer derivatives can detect Hg^{2+} in a HEPES buffer solution of pH 7.4 in a colorimetric fashion. But, interestingly, **76a** detected Hg^{2+} in ~60 minutes and **76b** in ~15 minutes at pH = 7.4. So the deprotection of dithioacetal promoted by Hg^{2+} was 4 times faster in the case of **76b** compared to **76a** due to the formation of C═O···Hg interaction, which further triggered the C···S–Hg cleavage which leads to aldehyde formation. But in the case of pH = 11, **76b** showed a ~60 minute reaction time in the presence of excess of Hg^{2+} ions, which suggested the pH-tunable sensitivity of the sensors. Ultimately the pH-dependent deprotection of dithioacetal was the main mechanism (Fig. 39) for the colorimetric detection ability of both sensors (**76a** and **76b**).

A set of sensors **77a** and **77b** were developed as PEGylated BODIPY polymers.[139] The presence of a dithia-dioxa-aza cyclopentadecane ligand to the BODIPY core triggered the ICT process and both sensors were non-emissive. Due to the presence of PEG units, **77a** and **77b** can be used for the detection of Hg^{2+} ions in pure water (Fig. 40). In the presence of Hg^{2+}, a drastic change in color and enhanced fluorescence were observed in both **77a** and **77b**. A yellow emission with a pink color to the naked eye for **77a** and red emission with blue color to the naked eye for **77b** were observed in the presence of Hg^{2+}. Complexation of Hg^{2+} with the dithia-dioxa-aza cyclopentadecane ligand leads to the color and emission change. Due to the intense and bright emissive nature of **77a** and **77b**, they can be used at the cellular level to detect Hg^{2+} ions. The LOD value for **77a** is 8.1 ppb and that for **77b** is 129.3 ppb.

A tryptophan-dithiocarbamate-based fluorogenic polymeric probe **78**[140] was developed for the selective detection and removal of Hg^{2+} ions. In pure aqueous medium, **78** was able to detect Hg^{2+} by an enhancement in fluorescence signal at 366 nm due to the inhibition of the PET process. Due to the presence of a dithiocarbamate unit, it can bind the Hg^{2+} ion and stop the PET process to give the fluorescence signal (Fig. 41). With a detection limit of 1.5 nM, sensor **78** is able to detect Hg^{2+} at the cellular level. Another water-soluble copolymer **79**[141] was developed with a tryptophan unit and a pyridine segment attached through an imine bond. Due to the complexation of Hg^{2+} through the N atoms of the imine bond and pyridine units, quenching of fluorescence was observed (Fig. 41). This quenched fluorescence of **79** was used to detect Hg^{2+} ions at the cellular level with an LOD value of 7.41 nM.

Another BODIPY-based thiosemicarbazone moiety containing polymeric sensor **80a**[142a] was developed for detecting Hg^{2+} ions in a pure aqueous (HEPES buffer solution, pH = 7.4) medium. Upon the addition of Hg^{2+}, a solution of **80a** showed yellow emission from fluorescence-off mode. The binding of Hg^{2+} ions with two thiosemicarbazone groups of nearby polymeric chains stopped the C═N isomerization and resulted in a yellow fluorescence (Fig. 42). Complexation of Hg^{2+} with **80a** resulted in a precipitate to remove Hg^{2+} successfully from the contaminated water source. Highly selective polymeric sensor **80a** has a detection limit of 0.36 μM and the capability to remove mercury.

For the first time a chitosan thiomer, **80b**[142b] has been synthesized successfully and applied for the colorimetric

Table 3 A comparison of different reaction-based sensors (**48–72**) for Hg^{2+} detection

Compound	Medium	LOD	Type of sensing	Biological study
48	PBS buffer (pH = 7.4, containing 2% DMSO)	7.6×10^{-9} M	Turn-on fluorescence	Done
49	EtOH–water (1 : 1, v/v)	1.03×10^{-8} M	Turn-on fluorescence	NA
50	THF–water (1 : 1, v/v, PBS, pH = 8.5)	1.59×10^{-8} M	Turn-on fluorescence	NA
51	THF–water (1 : 1, v/v)	3.1×10^{-7} M	Turn-on fluorescence	NA
52	PBS–DMSO buffer (5 : 5, v/v 20 mM, pH = 7.4)	6.8×10^{-8} M	Turn-on fluorescence and colorimetric	Done
53	Ethanol–HEPES buffer (1 : 1, v/v, pH = 7.4)	5.8×10^{-9} M	Turn-on fluorescence	NA
54a	MeCN–water (1 : 1, v/v)	57×10^{-9} M	Turn-on fluorescence	Done
54b	EtOH–H_2O (2 : 8, v/v, pH = 7.4)	4.0×10^{-8} M	Turn-on fluorescence	Done
54c	DMS–PBS buffer (1 : 99, v/v, pH = 7.4)	19.3×10^{-9} M	Turn-on fluorescence	Done
55	THF–PBS buffer (1 : 1, v/v, pH = 7.4)	59×10^{-9} M	Turn-on fluorescence	Done
56	PBS buffer	27×10^{-9} M	Turn-on fluorescence	NA
57	HEPES buffer	0.12×10^{-6} M	Turn-on fluorescence	NA
58	CH_3CN–PBS buffer (3 : 7, v/v, 10.0 mM, pH = 7.4)	244 ppb	Turn off fluorescence	NA
59	HEPES buffer	NA	Turn-on fluorescence and colorimetric	Done
60	Ethanol–H_2O (2 : 8, v/v 50 mM HEPES buffer solution, pH = 7.4)	3.2×10^{-9} M	Turn-on fluorescence	Done
61	PBS buffer (1% CH_3CN)	7.8×10^{-9} M	Turn-on fluorescence	Done
62	PBS buffer	6.5×10^{-9} M	Turn-on fluorescence	NA
63	HEPES buffer/DMSO (9 : 1, v/v, pH = 7.2)	70×10^{-9} M	Turn-on fluorescence	Done
64	CH_3CN/H_2O (8 : 2, v/v, 0.1 M $KClO_4$ buffer, pH = 7.34)	Nanomolar level	Turn-on fluorescence	Done
65	PBS/EtOH (9 : 1, v/v)	9.1×10^{-9} M	Ratiometric fluorescence	Done
66	EtOH–water (2 : 8, v/v)	18.8×10^{-9} M	Turn-on fluorescence	Done
67	MeCN–HEPES (1 : 9, v/v, pH = 7.2)	1.6×10^{-9} M	Turn-on fluorescence	Done
68a	MeCN–water (3 : 7, v/v)	1.08×10^{-6} M	Turn-on fluorescence	Done
68b	DMSO–water (1 : 9, v/v)	8.1×10^{-9} M	Colorimetric	NA
69	PBS buffer	300×10^{-12} M	Turn-on fluorescence	Done
70	HEPES buffer	40×10^{-9} M	Turn-on fluorescence	NA
71	EtOH–water (5/5, v/v, HEPES pH = 7.4)	55×10^{-9} M	Turn-on fluorescence	NA
72	CH_3CN–HEPES (10 mM, 1 : 4, v/v)	12×10^{-9} M	Turn-on fluorescence	Done

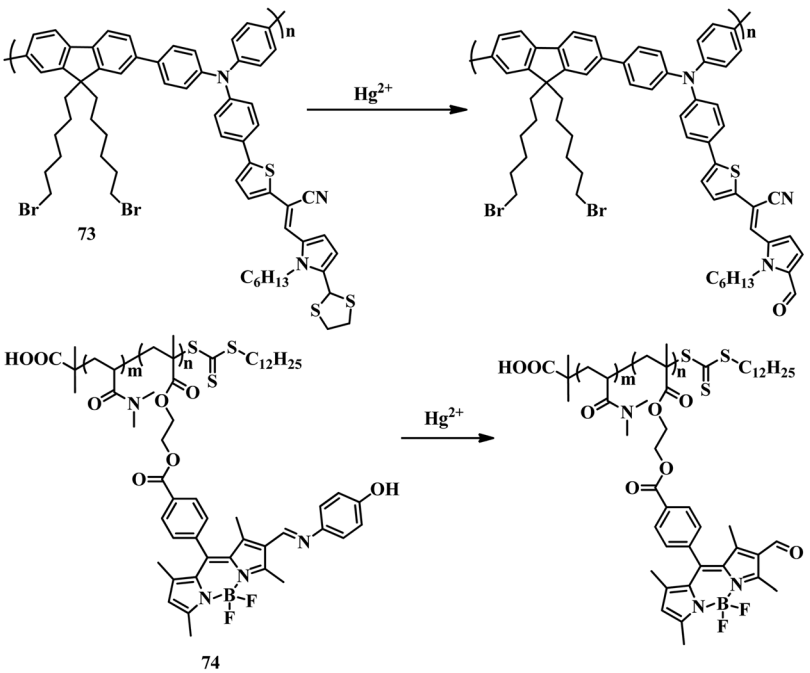

Fig. 38 The chemical structures and proposed sensing mechanisms of **73** and **74**.

detection of Hg^{2+} in aqueous solution. As Hg^{2+} has strong affinity towards thiol groups, **80b** turned out to be an excellent binding material for it. Due to the formation of an S–Hg–S bond (Fig. 42), a drastic change in colour is observed from colorless to yellow to light brown to brown. This polymeric material has also been applied for removal of Hg^{2+} ions due to strong

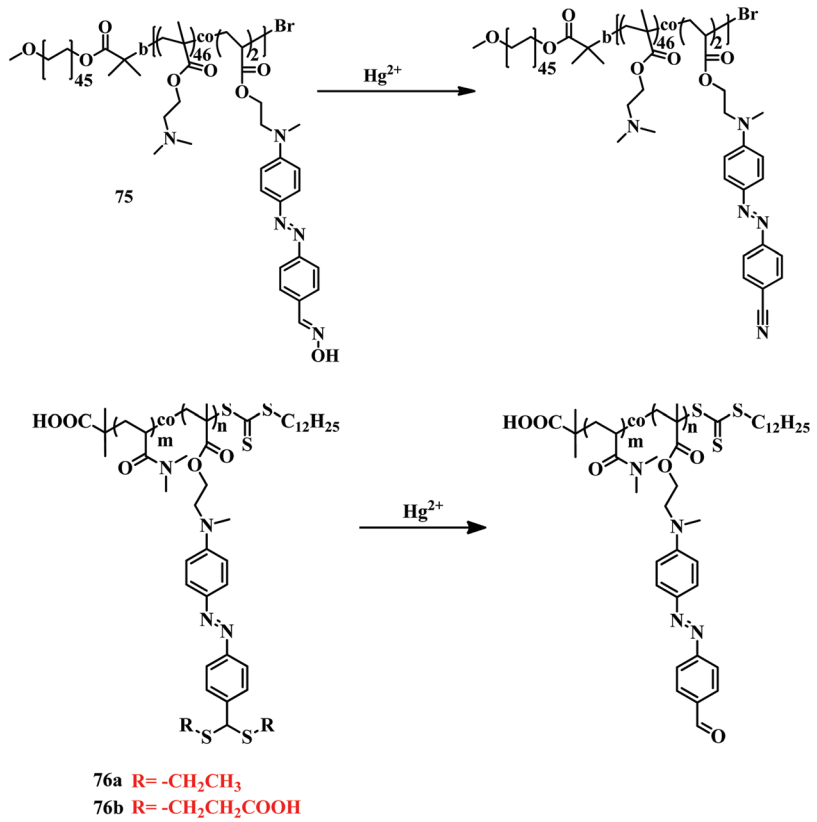

Fig. 39 The chemical structures and sensing mechanisms of sensors **75**, **76a**, and **76b**.

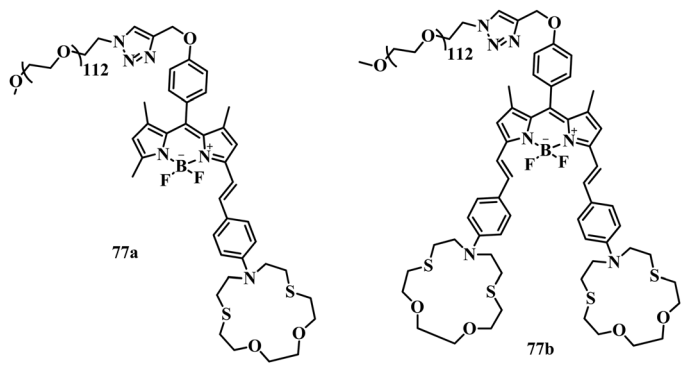

Fig. 40 The chemical structures of **77a** and **77b**.

binding. Polymer **80b** has been developed as an excellent sensor material with an ultra-low LOD of 0.465 ppb.

In this section, we have discussed polymeric sensors for the detection of Hg^{2+} ions. In recent years polymeric sensors have been developed to treat the analyte in pure water, which can be achieved by the synthesis of functionalized polymers with hydrophilic and hydrophobic segments. A summary of the information about polymeric sensors (**73–80b**) is given in Table 4.

We have now discussed the development and implementation of different types of detection systems based on heteroatom-containing ligand systems, reaction-based systems, and polymeric systems, for sensing Hg^{2+} ion in various sources.

3. Fluorescent and colorimetric detection systems for As(III)

The most toxic form of arsenic is the +3-oxidation state. In groundwater, arsenic exists as arsenite (As(III)) and arsenate (As(V)), though the arsenite form is more toxic than As(V). Except for conventional methods, rapid detection techniques using color change or emission change are very rare in number. In this section, we are going to discuss some of the chemical sensors which have been used to detect As(III) in a colorimetric way or a fluorometric way.

A combination of boron trifluoride diethyletherate ($(C_2H_5)_2OBF_3$) and curcumin produced sensor **81**[143] for the

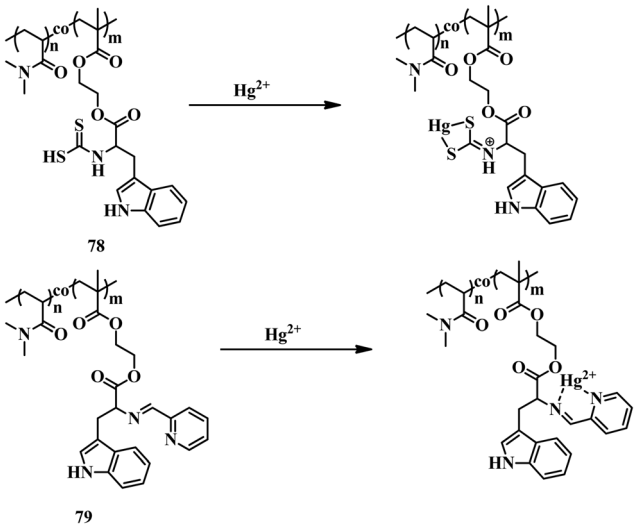

Fig. 41 The chemical structures and proposed sensing mechanisms of **78** and **79**.

selective detection of As(III) colorimetrically. A solution of **81** in 60% ethanol showed an orange color, but upon addition of As(III), it turned blue. This redshift in absorbance spectra was observed due to the deprotonation of the hydroxyl groups by As(III) to promote the delocalization of the negative charges towards the acceptor part (Fig. 43). This prominent change in color in the presence of As(III) can be used for the selective detection of As(III) with an LOD of 0.26 μM. Amberlite XAD-2 resin coated with **81** was used for the detection of As(III) in a solid phase with an LOD of 3×10^{-5} M.

Two isatin-appended Schiff bases **82a** and **82b**[144] were developed for the colorimetric detection of As(III). DMSO solutions of **82a** and **82b** showed a brown color but upon adding AsO_2^-, they turned blue with absorption maxima of 600 nm and 624 nm, respectively. The formation of a charge-transfer complex between As(III) and **82a**/**82b** resulted in the changed colors. For both sensors As(III) was bound through C═O and C═N segments, as depicted in Fig. 43. In a colorimetric fashion, **82a** and **82b** can be used as selective sensors for As(III) detection with detection limits of 0.26 ppm and 0.56 ppm.

Sensor **83**,[145] a combination of 2,6-diformyl-*p*-cresol and 4-aminoantipyrine was developed for the selective detection of arsenite in colorimetric and fluorometric fashion. A HEPES buffer (1 mM, pH 7.4; water/DMSO (v/v), 9 : 1) solution of **83** showed no color and no emission due to the strong PET effect originating from the hydroxyl group. Addition of AsO_3^{3-} ions to the solution of **83** produced a light-yellow greenish color and green emission. This drastic and prominent change in color and emission was the result of the binding of arsenite with **83**, which disturbed the PET process and triggered the CHEF process *via* intermolecular hydrogen bonding (Fig. 44). Its turn-on fluorescence feature was used effectively for intracellular tracking of arsenite. The dual-mode sensing process and excellent LOD value of 4.12 made **83** a potential tool in the field of rapid and effective arsenite detection.

Condensation between rhodamine 6G hydrazide and 5-methyl salicylaldehyde produced sensor **84**.[146] In acetonitrile : HEPES buffer (4 : 1, v/v, pH 7.4) solution, **84** did not show any color or emission due to the spirolactam ring-closed form. After the addition of As(III), a solution of **84** turned pink in color with an intense yellow emission. Spirolactam ring-opening followed by strong 1 : 1 binding between As(III) and **84** resulted in the observed color and emission change (Fig. 45). Due it turn-on fluorescence, **84** was also used for detecting As(III) at the cellular level. Dual-channel sensor **84** emerged as an excellent material for the selective detection of As(III) with an LOD of 0.164 ppb.

An aggregation-induced emission-based sensor **85** was developed using tetraphenylethene (TPE) as a fluorescent moiety and cysteine as a binding ligand for As(III).[147] An aqueous solution (THF–water, 1 : 99, v/v) of **85** (Fig. 45) was nonfluorescent, but upon addition of As(III) an intense blue fluorescence was observed and it gradually became more intense with an increasing concentration of As(III). Binding of As(III) with the –SH group of cysteine of **85** through the formation of As–S bond promoted the π–π stacking of TPE units to produce the intense blue emission which is typical of the AIE process. Sensor **85** has a detection limit of 0.5 ppb, which is much lower than the WHO limit.

An oxime-based fluorogenic probe **86**[148] was applied for the detection of arsenite with turn-on fluorescence. In a pure aqueous medium of pH 7.24, **86** did not show any prominent fluorescence signal, but upon the introduction of AsO_2^- a strong blue emission was observed. This turn-on fluorescence signal helped to detect AsO_2^- in pure aqueous medium with a detection limit of 1.32 μM.

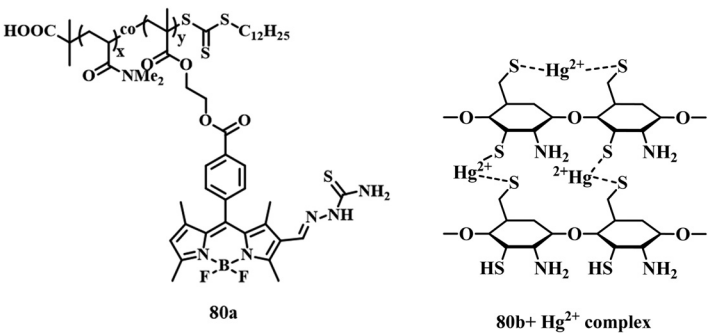

Fig. 42 The chemical structures of **80a** and **80b** + Hg^{2+} complex.

Table 4 A comparison of different polymer-based sensors (**73–80b**) for Hg^{2+} detection

Compound	Medium	LOD	Type of sensing	Biological study
73	THF	1×10^{-6} M	Turn-on fluorescence	NA
74	Pure water	1.1×10^{-6} M	Turn-on fluorescence	NA
75	Water	0.03×10^{-3} M	Colorimetric	NA
76a and **76b**	Pure water	NA	Colorimetric	NA
77a	Pure water	8.1 ppb	Turn-on fluorescence and colorimetric	Done
77b	Pure water	129.3 ppb	Turn-on fluorescence and colorimetric	Done
78	Pure water	1.5×10^{-9} M	Turn-on fluorescence	Done
79	Pure water	7.41×10^{-9} M	Turn-off fluorescence	Done
80a	HEPES buffer	0.37×10^{-6} M	Turn-on fluorescence	NA
80b	Aqueous medium	0.465 ppb	Colorimetric	NA

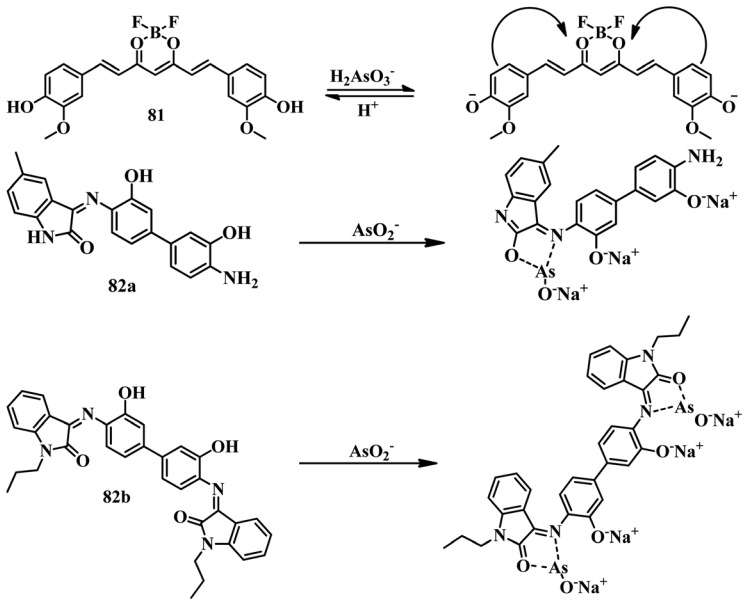

Fig. 43 The chemical structures and proposed sensing mechanisms of **81**, **82a**, and **82b**.

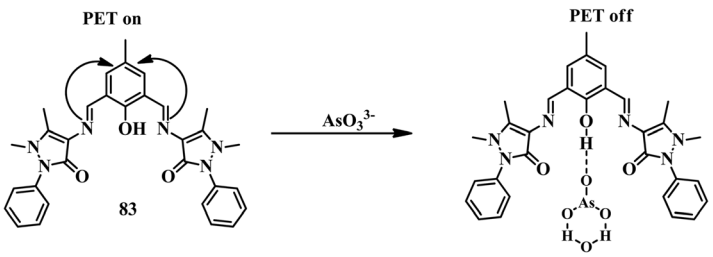

Fig. 44 The chemical structure and proposed sensing mechanism of sensor **83**.

The output fluorescence signal was the result of H-bonding interaction between AsO_2^- and **86** (Fig. 46). This H-bonding interaction leads to the formation of different nano/microstructures in pure aqueous solution. Sensor **86** was successfully utilized for cell imaging in the presence of AsO_2^- ions. This sensor suffered from a selectivity issue, as it showed similar fluorescence properties in the presence of arsenate as well. Along with the sensitivity issue, the LOD value of **86** towards AsO_2^- is not up to the mark compared to the WHO level.

A colorimetric probe **87** was designed as a benzothiazole Schiff base for the highly sensitive and selective detection of As^{3+} ions.[149] Sensor **87** showed a light yellow color in DMSO–water (1 : 1) medium. After the addition of As^{3+} ions, a solution of **87** turned brownish orange. Due to strong 1 : 1 binding between **87** and As^{3+} (Fig. 46), a strong change in color was observed. But unfortunately, the same characteristics were observed when **87** was treated with As^{5+} with the same absorbance spectrum. Though the drastic change in color was helpful for recognizing As^{3+} ions, the selectivity

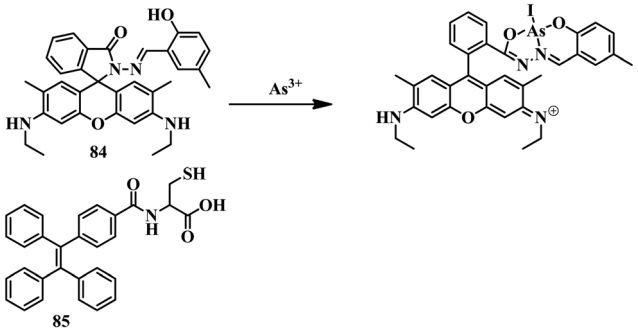

Fig. 45 The chemical structures of **84** and **85** along with the proposed sensing mechanism of **84**.

issue was a drawback for this system. It can be used for detecting arsenic (As^{3+}/As^{5+}) in water but cannot be used for the selective detection of As^{3+}. Sensor **87** suffered from selectivity issues, but the detection limit was excellent with an LOD value of 7.2 ppb for As^{3+} ions.

A chromogenic–fluorescence probe **88**[150] was applied for the detection of As^{3+} along with Cr^{3+}, Fe^{3+}, Al^{3+}, Ga^{3+}, and In^{3+} ions. In a water–MeCN (95 : 5, v/v) solution, in the presence of As^{3+}, the color of **88** changed to violet from colorless along with a quenching of fluorescence. For all other trivalent cations as well, the same observation was found. It was hypothesized that cation-induced dehydration formed a highly conjugated cationic molecule and that led to the color change (Fig. 47). Sensor **88** has LODs of 10.4 μM (UV-vis) and 10.7 μM (fluorescence). Though the color change is drastic in the case of **88**, it suffered from low selectivity towards As^{3+} and a low detection limit. Due to these issues, **88** cannot be used to separately detect As^{3+} ions. Similarly, another sensor **89** was developed by the combination of 2-hydroxy-1-naphthaldehyde and thiosemicarbazide.[151] With no color or emission in DMF–water (9 : 1, v/v, HEPES, pH = 7.2), **89** changed its color to yellow with a unique emission at 495 nm upon addition of AsO_2^- ions. A strong hydrogen bonding interaction between AsO_2^- and the –OH and –NH groups of **89** leads to a color and emission change (Fig. 47). Eventually, **89** could be a useful sensor with an LOD value of 66 nM but it suffers from the selectivity issue as it can also detect CN^- ions with the same spectroscopic properties.

Another hydrazine-based thiocarbamide chemosensor **90** was applied for the colorimetric and fluorometric detection of AsO_3^{3-} ions.[152] Sensor **90** detected AsO_3^{3-} ions in MeCN–water (9 : 1, v/v, pH = 7.2) by changing the color from colorless to yellow and non-

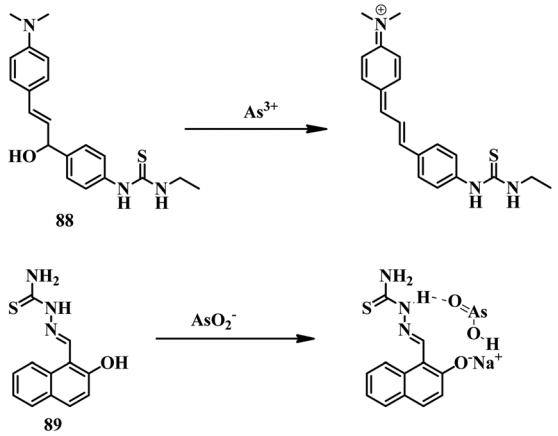

Fig. 47 The chemical structures and proposed sensing mechanisms of sensors **88** and **89**.

fluorescent to yellow fluorescence. Here also the H-bonding interaction between the anion, the –NH group of thiocarbamide segment, and the Ar–OH group was the reason behind the change in color as well as in fluorescence (Fig. 48). The dual-sensing properties of **90** with an excellent detection limit of 15 nM meant it emerged as a good tool for detecting As(III) in real applications as it was able to detect the analyte in contaminated real samples. It can also detect phosphate ions with the same color and emission change as AsO_3^{3-}, so there might be interference.

Another fluorogenic probe **91** was designed by the combination of pyrene and calix[4]arene for detecting As^{3+}.[153] Due to the presence of an amide group in the system, it can be a catalysis binding site as well as helping the CHEF process. In the presence of As^{3+} ions, the fluorescence intensity of **91** decreased, as a result of binding between the sensor and analyte for activation of the PET process (Fig. 48). This turn-off fluorescence of **91** was used to analyze real samples contaminated by As^{3+}, as the sensor has an LOD value of 11.53 nM for As^{3+}. Besides the excellent sensitivity of **91** towards As^{3+}, selectivity was a problem as the sensor was able to detect Nd^{3+} and Br^- by turn-on and turn-off fluorescence, respectively, under the same experimental conditions.

A colorimetric sensor **92** was developed with condensation between 2,4-dinitrophenyl hydrazine and 2,4-dihydroxy benzaldehyde.[154] Due to the presence of 2,4-dinitrophenyl hydrazine, it can act as an H-bonding formation segment with some unique chromophoric features. Sensor **92** (Fig. 49) showed different colors in water–DMSO (9 : 1) and water–MeCN

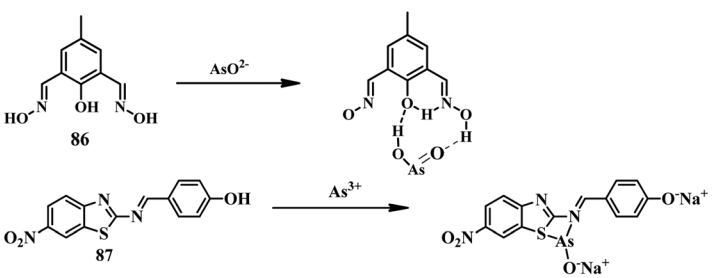

Fig. 46 The chemical structures and proposed sensing mechanisms of **86** and **87**.

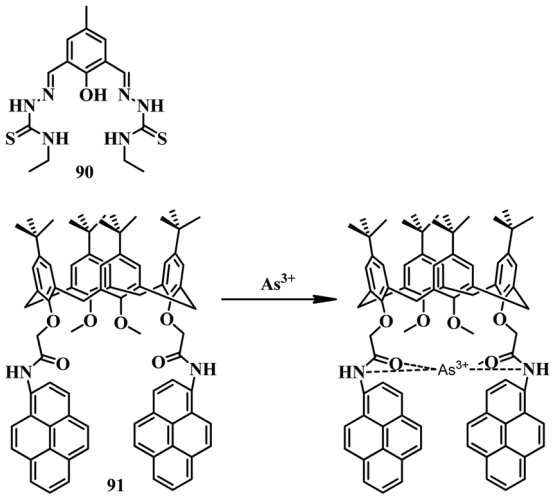

Fig. 48 The chemical structures of **90** and **91** along with the proposed sensing mechanism of **91**.

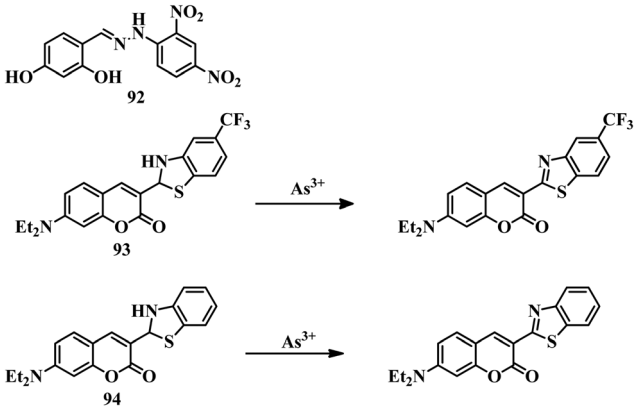

Fig. 49 The chemical structures of **92**, **93**, and **94**, and the proposed sensing mechanisms of **93** and **94**.

(9 : 1) mixtures. The color of **92** in water–DMSO solution changed to purple from orange in the presence of As^{3+} but in the case of a water–MeCN solution, it changed from yellow to red. The presence of Ar–OH and –NH groups in the sensor was attributed to the strong bonding of As^{3+} by H-bonding interaction which resulted in a drastic and intense color change. So, sensor **92** can serve as a good naked-eye sensor with high selectivity and an LOD value of 0.35×10^{-6} M for As^{3+} ions.

Two coumarin-based sensors **93**[155] and **94**[156] were designed as coumarin-appended benzothiazolines for the detection of As(III) in organic media. Both sensors were able to detect As(III) in THF medium by turn-on fluorescence. It was expected that As(III) coordination with the Schiff-base thiolate form of the sensors followed by the formation of benzothiazole was the reason behind the turning on of emission in both cases (Fig. 49). Both sensors were able to detect As(III) with high selectivity in pure THF medium. Sensor **94** was able to sense inorganic As(III) with an LOD value of 0.14 ppb. Similarly, sensor **93** was also extremely sensitive towards As(III) with a detection limit of 0.24 ppb. But both sensors were able to sense As(III) in an organic medium, which could be a drawback for them.

A norbornene-derived monomer **95a** and its homopolymer **95b** were developed for detecting As(III), where rhodamine B was used as the signaling unit.[157] Both the monomer and polymer solution in methanol–water solution remained colorless as well as non-emissive due to the spirolactam ring-closed form of the rhodamine unit. In the presence of KIO_3 and HCl, the solution of **95a** turned pink in color and reddish in emission due to the opening of the spirolactam ring. After the addition of As(III) solution, the pH changed from 1.34 to 4.23, and the color of the solution changed to brown, and the emission changed to greenish. In the presence of KIO_3 and HCl, As(III) oxidized to As(V) and generated I_2 in the solution. This I_2 further reacted with the double bond of the norbornene unit, and as a result, the color and fluorescence were changed (Fig. 50). A similar mechanism was followed by polymer **95b**.

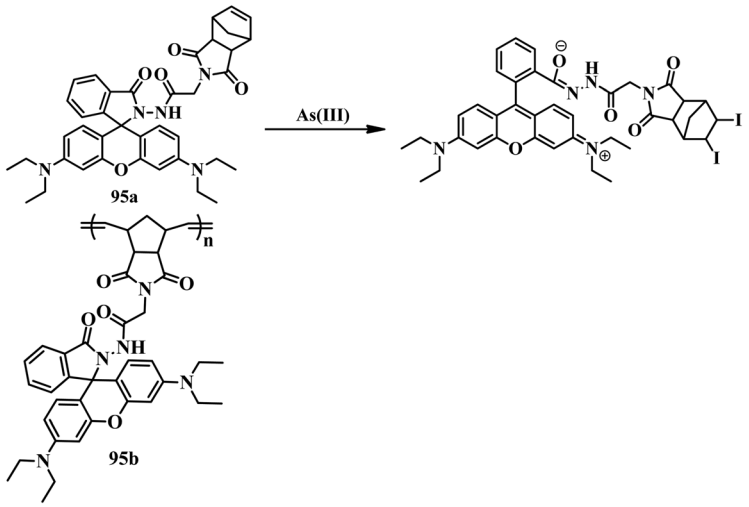

Fig. 50 The chemical structures of **95a** and **95b** along with the proposed sensing mechanism of **95a**.

Table 5 A comparison of different sensors (**81–95b**) for As(III) detection

Compound	Medium	LOD	Type of sensing	Biological study
81	60% ethanol	3×10^{-5} M	Colorimetric	NA
82a	DMSO	0.26 ppm	Colorimetric	NA
82b	DMSO	0.56 ppm	Colorimetric	NA
83	Water–DMSO (9 : 1, v/v, pH = 7.4)	4.12 ppb	Colorimetric and turn-on fluorescence	NA
84	MeCN–HEPES (4 : 1, v/v, pH = 7.4)	0.164 ppb	Colorimetric and turn-on fluorescence	Done
85	THF–water (1 : 99, v/v)	0.5 ppb	Turn-on fluorescence	NA
86	Pure aq. medium	1.32×10^{-6} M	Turn-on fluorescence	Done
87	DMSO–water (1 : 1, v/v)	7.2 ppb	Colorimetric	NA
88	Water–MeCN (95 : 5, v/v)	10.4×10^{-6} M (UV), 10.7×10^{-6} M (FL)	Colorimetric and turn-on fluorescence	NA
89	DMF–water (9 : 1, v/v, HEPES, pH = 7.2)	66×10^{-9} M	Colorimetric and turn-on fluorescence	NA
90	MeCN–water (9 : 1, v/v, pH = 7.2)	15×10^{-9} M	Turn-on fluorescence and colorimetric	NA
91	MeCN–PBS (8 : 2, v/v, pH = 7.2)	11.53×10^{-9} M	Turn-off fluorescence	NA
92	Water–DMSO (9 : 1, v/v)	0.35×10^{-6} M	Colorimetric	NA
93	THF	0.24 ppb	Turn-on fluorescence	NA
94	THF	0.14 ppb	Turn-on fluorescence	NA
95a	MeOH–water	200×10^{-9} M	Colorimetric and turn-on fluorescence	NA

The oxidation process was further supported by cyclic voltammetry which suggested that two-electron oxidation took place during the sensing process. Paper strips coated with polymer **95b** were successfully used for the ''in-field'' detection of As(III) in water sources. So it is clear that **95a** and **95b** are unique for their selective detection of As(III) in both colorimetric and fluorometric processes in a novel mechanistic pathway. Sensor **95a** has a detection limit of 200 nM for As(III) ions.

We have discussed reported chemical sensors for the detection of As(III) in different mediums with different mechanisms. Most of the sensors preferably interact with As(III) to produce a new signal for the identification of the analyte. All the information about sensors **81–95b** is given in Table 5.

4. Conclusions and perspectives

Due to the toxic extent of Hg^{2+} and As(III) in humans and in different biological systems, these ions have received extensive interest from researchers with the aim of creating detection tools. The initial section of our review covered reported colorimetric and fluorescence sensors for Hg^{2+} developed after 2015. Recognition of Hg^{2+} ions was achieved successfully by ligand-based systems and rhodamine systems; many of the systems suffered from selectivity issues, but most of them are reversible. This reversible nature can be used for the reuse of the sensor for detection purposes, which is a great advantage. These selectivity issues have been overcome by the development of reaction-based sensor systems where Hg^{2+}-mediated new molecule formation leads to output signals. Unfortunately, most of the small molecule sensors we have discussed here suffer from low solubility in water. Despite the solubility issues, many of these have excellent sensitivity, with LOD values lower than the permissible concentration of Hg^{2+} set by the EPA/WHO. However, solubility issues have been taken care of by introducing polymeric materials, where different hydrophilic segments were used to increase the water solubility of the sensors. Despite the water solubility of the polymeric materials, the sensitivity of these sensors is not up to the mark compared to small molecular sensors. Many of the discussed sensors were able to successfully track Hg^{2+} ions in biological systems with a distinct emission change, which is a new development in the field of mercury sensors. Apart from Hg^{2+}, some of the sensors discussed here can detect CH_3Hg^+ in both environmental samples and biological systems, which is an impressive development and opens up a new area for the design and development of new sensors. On the other hand, the development of As(III) ion sensors is still very rare due to their complicated chemical behavior. We have tried to cover most of the available chemical sensors for As(III) in this review. Most of the sensors for As(III) are based on H-bonding interactions, which leads to a color change or fluorescence change. Unfortunately, most of the discussed sensors suffer from interference from other trivalent metal ions or anions with the same output signal. This interference is harsh in the case of the distinct identification of As(III), either in cationic form or in anionic form. Apart from the selectivity viewpoint, most of the sensors have a detection limit way below the WHO/EPA guidelines.

For both toxic ions, different new methods have been developed in the last decade with new strategies, new applications, *etc.* We believe that in the case of Hg^{2+} ion detection, polymeric sensors can evolve as an excellent system due to their many advantages, such as signal amplification (as many repeating units are present), water solubility, and the stability of the probes. The detection limits should be improved for better implementation of ''in-field'' applications of polymeric materials. On the other hand, in the area of As(III) detection, there is a huge chance for improvement with respect to the design and development of sensors. For a more useful toolkit for As(III) detection, highly selective and sensitive sensors are in high demand to date. More and more development of polymeric sensors for As(III) detection is needed for device fabrication to provide a permanent solution for societies that are greatly affected by arsenic poisoning.

List of abbreviations

LED	Light-emitting diode
DMF	Dimethylformamide

DMSO	Dimethyl sulfoxide
THF	Tetrahydrofuran
UV-vis	Ultraviolet-visible
LCST	Lower critical solution temperature
HEPES	4-(2-Hydroxyethyl)piperazine-1-ethanesulfonic acid
PBS	Phosphate-buffered saline
BODIPY	Boron-dipyrromethene
NBD	7-Nitrobenz-2-oxa-1,3-diazole
NIR	Near-infrared
ICT	Intramolecular charge transfer
PET	Photoinduced electron transfer
FRET	Förster resonance energy transfer
ESIPT	Excited-state intramolecular proton transfer
AIEE	Aggregation induced enhanced emission
AIE	Aggregation induced emission
CHEF	Chelation-enhanced fluorescence
TICT	Twisted intramolecular charge transfer

Conflicts of interest

There are no conflicts to declare.

Acknowledgements

T. S. thanks IISER Kolkata for a research fellowship. R. S. thanks DST, DBT, IISER Kolkata for funding. T. S. and R. S. thank IISER Kolkata for infrastructure support.

References

1 G. Banfalvi, *Cellular Effects of Heavy Metals*, Springer, Netherlands, London, New York, 2011.
2 N. Herawati, S. Suzuki, K. Hayashi, I. F. Rivai and H. Koyoma, Cadmium, copper and zinc levels in rice and soil of Japan, Indonesia and China by soil type, *Bull. Environ. Contam. Toxicol.*, 2000, **64**, 33–39.
3 S. Sarkar and R. Shunmugam, Unusual redshift of the sensor while detecting the presence of Cd^{2+} in aqueous environment, *ACS Appl. Mater. Interfaces*, 2013, **5**, 7379–7383.
4 W. Salomons, U. Forstner and P. Mader, *Heavy Metals: Problems and Solutions*, Springer-Verlag, Berlin, Germany, 1995.
5 S. Bhattacharya, V. N. Rao, S. Sarkar and R. Shunmugam, Unusual emission from norbornene derived phosphonate molecule-a sensor for Fe^{III} in aqueous environment, *Nanoscale*, 2012, **4**, 6962–6966.
6 World Health Organization, *Guidelines for drinking-water quality*, Geneva, 3rd edn, 2004, vol. 1, p. 188.
7 P. B. Tchounwou, C. G. Yedjou, A. K. Patlolla and D. J. Sutton, Heavy metal toxicity and the environment, *Molecular, clinical and environmental toxicology*, Springer, Basel, 2012, pp. 133–164.
8 (*a*) J. C. Saha, A. K. Dikshit, M. Bandyopadhyay and K. C. Saha, A review of arsenic poisoning and its effects on human health, *Crit. Rev. Environ. Sci. Technol.*, 1999, **29**, 281–313; (*b*) K. Christen, *Environ. Sci. Technol*, 2001, **35**, 184–185.
9 S. Kapaj, H. Peterson, K. Liber and P. Bhattacharya, Human Health Effects from Chronic Arsenic Poisoning – A Review, *J. Environ. Sci. Health, Part A: Toxic/Hazard. Subst. Environ. Eng.*, 2006, **41**, 2399–2428.
10 K. S. M. Abdul, S. S. Jayasinghe, E. P. Chandana, C. Jayasumana and P. M. C. De Silva, Arsenic and human health effects: A review, *Environ. Toxicol. Pharmacol.*, 2015, **40**, 828–846.
11 A. H. Smith, C. Hopenhayn-Rich, M. N. Bates, H. M. Goeden, I. Hertz-Picciotto, H. M. Duggan, R. Wood, M. J. Kosnett and M. T. Smith, Cancer risks from arsenic in drinking water, *Environ. Health Perspect.*, 1992, **97**, 259–267.
12 W. R. Cullen and K. J. Reimer, Arsenic speciation in the environment, *Chem. Rev.*, 1989, **89**, 713–764.
13 N. Bhandari, R. J. Reeder and D. R. Strongin, Photoinduced oxidation of arsenite to arsenate in the presence of goethite, *Environ. Sci. Technol.*, 2012, **46**, 8044–8051.
14 United States Environmental Protection Agency Arsenic and Clarifications to Compliance and New Source Monitoring Rule: A Quick Reference Guide, EPA 816-F-01-004, US EPA, Wasington, D.C., 2001.
15 B. Weiss, Why methylmercury remains a conundrum 50 years after Minamata, *Toxicol. Sci*, 2007, **97**, 223–225.
16 L. Amin-Zaki, S. Elhassani, M. A. Majeed, T. W. Clarkson, R. A. Doherty and M. Greenwood, Intra-uterine methylmercury poisoning in Iraq, *Problems of Birth Defects*, Springer, Dordrecht, 1974, pp. 233–241.
17 F. Di Natale, A. Lancia, A. Molino, M. Di Natale, D. Karatza and D. Musmarra, Capture of mercury ions by natural and industrial materials, *J. Hazard. Mater.*, 2006, **132**, 220–225.
18 W. F. Fitzgerald, C. H. Lamborg and C. R. Hammerschmidt, Marine biogeochemical cycling of mercury, *Chem. Rev.*, 2007, **107**, 641.
19 T. W. Clarkson, L. Magos and G. J. Myers, The toxicology of mercury-current exposures and clinical manifestations, *N. Engl. J. Med.*, 2003, **349**, 1731–1737.
20 R. Von Burg, Inorganic mercury, *J. Appl. Toxicol.*, 1995, **15**, 483–493.
21 R. Shunmugam, G. J. Gabriel, C. E. Smith, K. A. Aamer and G. N. Tew, A highly selective colorimetric aqueous sensor for mercury, *Chem. – Eur. J.*, 2008, **14**, 3904–3907.
22 J. Chen, J. Pan and S. Chen, A Naked-Eye Colorimetric Sensor for Hg^{2+} Monitoring with Cascade Signal Amplification Based on Target Induced Conjunction of Split DNAzyme Fragments, *Chem. Commun.*, 2017, **53**, 10224–10227.
23 V. Iyengar and J. Woittiez, Trace elements in human clinical specimens: evaluation of literature data to identify reference values, *Clin. Chem.*, 1988, **34**, 474–481.
24 A. T. Townsend, K. A. Miller, S. McLean and S. Aldous, The determination of copper, zinc, cadmium and lead in urine

by high resolution ICP-MS, *J. Anal. At. Spectrom.*, 1998, **13**, 1213–1219.

25 X. C. Le, M. Ma and N. A. Wong, Speciation of arsenic compounds using high-performance liquid chromatography at elevated temperature and selective hydride generation atomic fluorescence detection, *Anal. Chem.*, 1996, **68**, 4501–4506.

26 C. B'Hymer and J. A. Caruso, Arsenic and its speciation analysis using high-performance liquid chromatography and inductively coupled plasma mass spectrometry, *J. Chromatogr. A*, 2004, **1045**, 1–13.

27 K. C. Thompson and R. J. Reynolds, *Atomic Absorption. Fluorescence and Flame Emission Spectroscopy*, Charles Griffin, London, 2nd edn, 1978, vol. 51, pp. 175–176.

28 J. L. Gomez-Ariza, D. Sánchez-Rodas, I. Giráldez and E. Morales, A comparison between ICP-MS and AFS detection for arsenic speciation in environmental samples, *Talanta*, 2000, **51**, 257–268.

29 T. Nakazato and H. Tao, A high-efficiency photooxidation reactor for speciation of organic arsenicals by liquid chromatography – hydride generation – ICPMS, *Anal. Chem.*, 2006, **78**, 1665–1672.

30 M. Mulvihill, A. Tao, K. Benjauthrit, J. Arnold and P. Yang, Surface-enhanced Raman spectroscopy for trace arsenic detection in contaminated water, *Angew. Chem.*, 2008, **120**, 6556–6560.

31 H. M. Anawar, Arsenic Speciation in Environmental Samples by Hydride Generation and Electrothermal Atomic Absorption Spectrometry, *Talanta*, 2012, **88**, 30–42.

32 W. Holak, Determination of Arsenic by Cathodic Stripping Voltammetry with a Hanging Mercury Drop Electrode, *Anal. Chem.*, 1980, **52**, 2189–2192.

33 S. S. Hassan, A. R. Sirajuddin, T. G. Solangi, M. S. Kazi, Y. Kalhoro, Z. Junejo, A. Tagar and N. H. Kalwar, Nafion Stabilized Ibuprofen-Gold Nanostructures Modified Screen Printed Electrode as Arsenic(III) Sensor, *J. Electroanal. Chem.*, 2012, **682**, 77–82.

34 Y. Zhou, Z. Xu and J. Yoon, Fluorescent and colorimetric chemosensors for detection of nucleotides, FAD and NADH: highlighted research during 2004–2010, *Chem. Soc. Rev.*, 2011, **40**, 2222–2235.

35 D. T. Quang and J. S. Kim, Fluoro-and chromogenic chemodosimeters for heavy metal ion detection in solution and biospecimens, *Chem. Rev.*, 2010, **110**, 6280–6301.

36 X. Chen, Y. Zhou, X. Peng and J. Yoon, Fluorescent and colorimetric probes for detection of thiols, *Chem. Soc. Rev.*, 2010, **39**, 2120–2135.

37 J. F. Zhang, Y. Zhou, J. Yoon and J. S. Kim, Recent progress in fluorescent and colorimetric chemosensors for detection of precious metal ions (silver, gold and platinum ions), *Chem. Soc. Rev.*, 2011, **40**, 3416–3429.

38 E. M. Nolan and S. J. Lippard, Tools and tactics for the optical detection of mercuric ion, *Chem. Rev.*, 2008, **108**, 3443–3480.

39 H. N. Kim, W. X. Ren, J. S. Kim and J. Yoon, Fluorescent and colorimetric sensors for detection of lead, cadmium, and mercury ions, *Chem. Soc. Rev.*, 2012, **41**, 3210–3244.

40 G. Chen, Z. Guo, G. Zeng and L. Tang, Fluorescent and colorimetric sensors for environmental mercury detection, *Analyst*, 2015, **140**, 5400–5443.

41 M. B. Gumpu, S. Sethuraman, U. M. Krishnan and J. B. B. Rayappan, A review on detection of heavy metal ions in water–an electrochemical approach, *Sens. Actuators, B*, 2015, **213**, 515–533.

42 M. Mulvihill, A. Tao, K. Benjauthrit, J. Arnold and P. Yang, Surface-enhanced Raman spectroscopy for trace arsenic detection in contaminated water, *Angew. Chem., Int. Ed.*, 2008, **47**, 6456–6460.

43 J. Hao, M. J. Han, S. Han, X. Meng, T. L. Su and Q. K. Wang, SERS detection of arsenic in water: A review, *J. Environ. Sci.*, 2015, **36**, 152–162.

44 E. Priyadarshini and N. Pradhan, Gold nanoparticles as efficient sensors in colorimetric detection of toxic metal ions: a review, *Sens. Actuators, B*, 2017, **238**, 888–902.

45 M. Li, H. Gou, I. Al-Ogaidi and N. Wu, Nanostructured sensors for detection of heavy metals: a review, *ACS Sustainable Chem. Eng.*, 2013, **1**, 713–723.

46 L. Farzin, M. Shamsipur and S. Sheibani, A review: Aptamer-based analytical strategies using the nanomaterials for environmental and human monitoring of toxic heavy metals, *Talanta*, 2017, **174**, 619–627.

47 A. Maity, A. Sil, S. Nad and S. K. Patra, A highly selective, sensitive and reusable BODIPY based 'OFF/ON'fluorescence chemosensor for the detection of Hg^{2+} Ions, *Sens. Actuators, B*, 2018, **255**, 299–308.

48 C. B. Bai, P. Xu, J. Zhang, R. Qiao, M. Y. Chen, M. Y. Mei, B. Wei, C. Wang, L. Zhang and S. S. Chen, Long-Wavelength Fluorescent Chemosensors for Hg^{2+} based on Pyrene, *ACS Omega*, 2019, **4**, 14621–14625.

49 A. Kumar, R. Ananthakrishnan, G. Jana, P. K. Chattaraj, S. Nayak and S. K. Ghosh, An Intramolecular Charge Transfer Induced Fluorescent Chemosensor for Selective Detection of Mercury (II) and its Self-Turn-On Inside Live Cells at Physiological pH, *ChemistrySelect*, 2019, **4**, 4810–4819.

50 B. Muzey and A. Naseem, An AIEE active 1, 8-naphthalimide-sulfamethizole probe for ratiometric fluorescent detection of Hg^{2+} ions in aqueous media, *J. Photochem. Photobiol., A*, 2020, **391**, 112354.

51 Y. Yuan, X. Chen, Q. Chen, G. Jiang, H. Wang and J. Wang, New switch on fluorescent probe with AIE characteristics for selective and reversible detection of mercury ion in aqueous solution, *Anal. Biochem.*, 2019, **585**, 113403.

52 T. P. Yoon and E. N. Jacobsen, Privileged chiral catalysts, *Science*, 2003, **299**, 1691–1693.

53 A. Dalla Cort, P. De Bernardin, G. Forte and F. Y. Mihan, Metal–salophen-based receptors for anions, *Chem. Soc. Rev.*, 2010, **39**, 3863–3874.

54 K. Liu, Y. Zhang, T. Zhou, X. Liu, B. Chen, X. Wang, X. Zhao, J. Huo, Y. Wang and B. Zhu, Sequential recognition of Hg^{2+} and I^- based on a novel BODIPY-salen sensor, *Sens. Actuators, B*, 2017, **253**, 1194–1198.

55 N. Dey, J. Kulhanek, F. Bures and S. Bhattacharya, *J. Org. Chem.*, 2019, **84**, 1787–1796.

56 Y. Li, W. Shi, J. Ma, X. Wang, X. Kong, Y. Zhang, L. Feng, Y. Hui and Z. Xie, A novel optical probe for Hg^{2+} in aqueous media based on mono-thiosemicarbazone Schiff base, *J. Photochem. Photobiol., A*, 2017, **338**, 1–7.

57 A. Kumar and N. Ahmed, Indirect Approach for CN–Detection: Development of ''Naked-Eye'' Hg^{2+}-Induced Turn-Off Fluorescence and Turn-On Cyanide Sensing by the Hg^{2+} Displacement Approach, *Ind. Eng. Chem. Res.*, 2017, **56**, 6358–6368.

58 K. M. Vengaian, C. D. Britto, K. Sekar, G. Sivaraman and S. Singaravadivel, Phenothiazine-diaminomalenonitrile based Colorimetric and Fluorescence ''Turn-off-on'' Sensing of Hg^{2+} and S^{2-}, *Sens. Actuators, B*, 2016, **235**, 232–240.

59 L. N. Neupane, P. K. Mehta, J. U. Kwon, S. H. Park and K. H. Lee, Selective red-emission detection for mercuric ions in aqueous solution and cells using a fluorescent probe based on an unnatural peptide receptor, *Org. Biomol. Chem.*, 2019, **17**, 3590–3598.

60 M. L. Presti, R. Martínez-Máñez, J. V. Ros-Lis, R. M. Batista, S. P. Costa, M. M. M. Raposo and F. Sancenón, A dual channel sulphur-containing a macrocycle functionalised BODIPY probe for the detection of Hg (II) in a mixed aqueous solution, *New J. Chem.*, 2018, **42**, 7863–7868.

61 A. K. Jha, S. Umar, R. K. Arya, D. Datta and A. Goel, Pyrano [3, 2-c] julolidin-2-ones: a novel class of fluorescent probes for ratiometric detection and imaging of Hg 2+ in live cancer cells, *J. Mater. Chem. B*, 2016, **4**, 4934–4940.

62 R. X. Zhang, P. F. Li, W. J. Zhang, N. Li and N. Zhao, A highly sensitive fluorescent sensor with aggregation-induced emission characteristics for the detection of iodide and mercury ions in aqueous solution, *J. Mater. Chem. C*, 2016, **4**, 10479–10485.

63 A. Tang, Z. Chen, D. Deng, G. Liu, Y. Tu and S. Pu, Aggregation-induced emission enhancement (AIEE)-active tetraphenylethene (TPE)-based chemosensor for Hg^{2+} with solvatochromism and cell imaging characteristics, *RSC Adv.*, 2019, **9**, 11865–11869.

64 S. Gharami, K. Aich, P. Ghosh, L. Patra, N. Murmu and T. K. Mondal, A fluorescent ''ON–OFF–ON'' switch for the selective and sequential detection of Hg^{2+} and I^- with applications in imaging using human AGS gastric cancer cells, *Dalton Trans.*, 2020, **49**, 187–195.

65 Y. F. Xiao, L. Yu and B. Quan, A highly selective and sensitive fluorescein-based chemodosimeter for Hg^{2+} ions in aqueous media, *Anal. Chim. Acta*, 2007, **584**, 95–100.

66 K. M. K. Swamy, K. K. Soo, L. N. Ha, K. S. M. Shantha, K. S. Jong and Y. Juyoung, Fluorescent sensing of pyrophosphate and ATP in 100% aqueous solution using a fluorescein derivative and Mn^{2+}, *Tetrahedron Lett.*, 2007, **48**, 8683–8686.

67 K. J. Hee, P. E. Ji, C. G. Myung, A. Sangdoo and C. K. Suk, Selective chromogenic and fluorogenic signalling of Hg^{2+} ions using a fluorescein-coumarin conjugate, *Dyes Pigm.*, 2010, **84**, 54–58.

68 P. Piyanuch, S. Watpathomsub, V. S. Lee, H. A. Nienaber and N. Wanichacheva, Highly sensitive and selective Hg^{2+}-chemosensor based on dithia-cyclic fluorescein for optical and visual-eye detections in aqueous buffer solution, *Sens. Actuators, B*, 2016, **224**, 201–208.

69 R. V. Rathod, S. Bera, P. Maity and D. Mondal, Mechanochemical Synthesis of a Fluorescein-Based Sensor for the Selective Detection and Removal of Hg^{2+} Ions in Industrial Effluents, *ACS Omega*, 2020, **5**, 4982–4990.

70 H. Mohammad, A. S. M. Islam, C. Prodhan and M. Ali, A fluorescein-based chemosensor for ''turn-on'' detection of Hg^{2+} and the resultant complex as a fluorescent sensor for S^{2-} in semi-aqueous medium with cell-imaging application: experimental and computational studies, *New J. Chem.*, 2019, **43**, 5297–5307.

71 N. Kaur, G. Jindal and S. Kumar, Cascade recognition of Hg^{2+} and cysteine using a naphthalene based ESIPT sensor and its application in a set/reset memorized device, *New J. Chem.*, 2019, **43**, 436–443.

72 J. Wang, Q. Rao, H. Wang, Q. Zhang, G. Liu, Z. Wu, J. Yu, X. Zhu, Y. Tian and H. Zhou, A terpyridine-based test strip for the detection of Hg^{2+} in various water samples and drinks, *Anal. Methods*, 2019, **11**, 227–231.

73 P. G. Sutariya, H. Soni, S. A. Gandhi and A. Pandya, Luminescent behavior of pyrene-allied calix [4] arene for the highly pH-selective recognition and determination of Zn^{2+}, Hg^{2+} and I^- via the CHEF-PET mechanism: computational experiment and paper-based device, *New J. Chem.*, 2019, **43**, 9855–9864.

74 T. Anand and S. K. Sahoo, Cost-effective approach to detect Cu (II) and Hg (II) by integrating a smartphone with the colorimetric response from a NBD-benzimidazole based dyad, *Phys. Chem. Chem. Phys.*, 2019, **21**, 11839–11845.

75 X. Cao, Y. Li, Y. Yu, S. Fu, A. Gao and X. Chang, *Nanoscale*, 2019, **11**, 10911–10920.

76 D. Liu, H. Zhu, J. Shi, X. Deng, T. Zhang, Y. Zhao, P. Qi, G. Yang and H. He, A 1, 8-naphthalimide-based fluorescent sensor with high selectivity and sensitivity for Hg^{2+} in aqueous solution and living cells, *Anal. Methods*, 2019, **11**, 3150–3154.

77 Y. Zhang, C. Zhang, Y. Wu, B. Zhao, L. Wang and B. Song, *RSC Adv.*, 2019, **9**, 23382–23389.

78 S. Srivastava, N. Thakur, A. Singh, P. Shukla, V. K. Maikhuri, N. Garg, A. Prasad and R. Pandey, Development of a fused imidazo [1,2-a] pyridine based fluorescent probe for Fe^{3+} and Hg^{2+} in aqueous media and HeLa cells, *RSC Adv.*, 2019, **9**, 29856–29863.

79 S. Sahana, G. Mishra, S. Sivakumar and P. K. Bharadwaj, A 2-(2′-hydroxyphenyl) benzothiazole (HBT)–quinoline conjugate: a highly specific fluorescent probe for Hg^{2+} based on ESIPT and its application in bioimaging, *Dalton Trans.*, 2015, **44**, 20139–20146.

80 F. Bu, B. Zhao, W. Kan, L. Ding, T. Liu, L. Wang, B. Song, W. Wang and Q. Deng, An ESIPT characteristic ''turn-on'' fluorescence sensor for Hg^{2+} with large Stokes shift and sequential ''turn-off'' detection of S^{2-} as well as the application in living cells, *J. Photochem. Photobiol., A*, 2020, **387**, 112165.

81 L. Zong, C. Wang, Y. Song, Y. Xie, P. Zhang, Q. Peng, Q. Li and Z. Li, A dual-function probe based on naphthalene diimide for fluorescent recognition of Hg^{2+} and colorimetric detection of Cu^{2+}, *Sens. Actuators, B*, 2017, **252**, 1105–1111.

82 L. Zong, Y. Xie, Q. Li and Z. Li, A new red fluorescent probe for Hg^{2+} based on naphthalene diimide and its application in living cells, reversibility on strip papers, *Sens. Actuators, B*, 2017, **238**, 735–743.

83 M. D. Gholami, S. Manzhos, P. Sonar, G. A. Ayoko and E. L. Izake, Dual chemosensor for the rapid detection of mercury (ii) pollution and biothiols, *Analyst*, 2019, **144**, 4908–4916.

84 P. Wang, Y. An and J. Wu, Highly sensitive turn-on detection of mercury (II) in aqueous solutions and live cells with a chemosensor based on tyrosine, *Spectrochim. Acta, Part A*, 2020, **230**, 118004.

85 J. C. Qin, J. Yan, B. D. Wang and Z. Y. Yang, Rhodamine–naphthalene conjugate as a novel ratiometric fluorescent probe for recognition of Al^{3+}, *Tetrahedron Lett.*, 2016, **57**, 1935–1939.

86 K. Wechakorn, K. Suksen, P. Piyachaturawat and P. Kongsaeree, Rhodamine-based fluorescent and colorimetric sensor for zinc and its application in bioimaging, *Sens. Actuators, B*, 2016, **228**, 270–277.

87 M. Devi, A. Dhir and C. P. Pradeep, A sandwich-type zinc complex from a rhodamine dye based ligand: a potential fluorescent chemosensor for acetate in human blood plasma and a molecular logic gate with INHIBIT function, *New J. Chem.*, 2016, **40**, 1269–1277.

88 Y. Wang, H. Q. Chang, W. N. Wu, X. L. Zhao, Y. Yang, Z. Q. Xu, Z. H. Xu and L. Jia, Rhodamine-2-thioxoquinazolin-4-one conjugate: a highly sensitiveandselective chemosensor for Fe3 + ions and crystal structures of its Ag(I) and Hg(II) complexes, *Sens. Actuators, B*, 2017, **239**, 60–68.

89 Y. L. Lin, R. Sung and K. Sung, Bis(rhodamine)-based polyether type of turn-on fluorescent sensors: selectively sensing Fe(III), *Tetrahedron*, 2016, **72**, 5744–5748.

90 J. Kuchlyan, S. Basak, D. Dutta, A. K. Das, D. Mal and N. Sarkar, A new rhodamine derived fluorescent sensor: Detection of Hg^{2+} at cellular level, *Chem. Phys. Lett.*, 2017, **673**, 84–88.

91 S. Hazra, C. Bodhak, S. Chowdhury, D. Sanyal, S. Mandal, K. Chattopadhyay and A. Pramanik, A novel tryptamine-appended rhodamine-based chemosensor for selective detection of Hg^{2+} present in aqueous medium and its biological applications, *Anal. Bioanal. Chem.*, 2019, **411**, 1143–1157.

92 Y. Wang, H. Ding, Z. Zhu, C. Fan, Y. Tu, G. Liu and S. Pu, Selective rhodamine–based probe for detecting Hg^{2+} and its application as test strips and cell staining, *J. Photochem. Photobiol., A*, 2020, **390**, 112302.

93 Y. Fang, X. Li, J.-Y. Li, G.-Y. Wang, Y. Zhou, N.-Z. Xu, Y. Hu and C. Yao, *Sens. Actuators, B*, 2018, **255**, 1182–1190.

94 G. Singh, S. I. Reja, V. Bhalla, D. Kaur, P. Kaur, S. Arora and M. Kumar, Hexaphenylbenzene appended AIEE active FRET based fluorescent probe for selective imaging of Hg^{2+} ions in MCF-7 cell lines, *Sens. Actuators, B*, 2017, **249**, 311–320.

95 M. She, S. Wu, Z. Wang, S. Ma, Z. Yang, B. Yin, P. Liu, S. Zhang and J. Li, Exploration of congeneric Hg (II)-mediated chemosensors driven by S-Hg affinity, and their application in living system, *Sens. Actuators, B*, 2017, **247**, 129–138.

96 P. Venkatesan, N. Thirumalivasan and S. P. Wu, A Rhodamine-based chemosensor with diphenylselenium for highly selective fluorescence turn-on detection of Hg^{2+} *in vitro* and *in vivo*, *RSC Adv.*, 2017, **7**, 21733–21739.

97 G. Yang, X. Meng, S. Fang, H. Duan, L. Wang and Z. Wang, A highly selective colorimetric fluorescent probe for detection of Hg^{2+} and its application on test strips, *RSC Adv.*, 2019, **9**, 8529–8536.

98 M. Hong, Y. Chen, Y. Zhang and D. Xu, A novel rhodamine-based Hg^{2+} sensor with a simple structure and fine performance, *Analyst*, 2019, **144**, 7351–7358.

99 M. Ozdemir, A rhodamine-based colorimetric and fluorescent probe for dual sensing of Cu^{2+} and Hg^{2+} ions, *J. Photochem. Photobiol., A*, 2016, **318**, 7–13.

100 S. Erdemir, M. Yuksekogul, S. Karakurt and O. Kocyigit, Dual-channel fluorescent probe based on bisphenol A-rhodamine for Zn^{2+} and Hg^{2+} through different signaling mechanisms and its bioimaging studies, *Sens. Actuators, B*, 2017, **241**, 230–238.

101 D. Cheng, W. Zhao, H. Yang, Z. Huang, X. Liu and A. Han, Detection of Hg^{2+} by a FRET ratiometric fluorescent probe based on a novel BODIPY-RhB system, *Tetrahedron Lett.*, 2016, **57**, 2655–2659.

102 M. Hong, S. Lu, F. Lv and D. Xu, A novel facilely prepared rhodamine-based Hg^{2+} fluorescent probe with three thiourea receptors, *Dyes Pigm.*, 2016, **127**, 94–99.

103 C. Kan, X. Shao, F. Song, J. Xu, J. Zhu and L. Du, Bioimaging of a fluorescence rhodamine-based probe for reversible detection of Hg (II) and its application in real water environment, *Microchem. J.*, 2019, **150**, 104142.

104 B. Gu, L. Huang, W. Su, X. Duan, H. Li and S. Yao, A benzothiazole-based fluorescent probe for distinguishing and bioimaging of Hg^{2+} and Cu^{2+}, *Anal. Chim. Acta*, 2017, **954**, 97.

105 L. Lan, Q. Niu and T. Li, A highly selective colorimetric and ratiometric fluorescent probe for instantaneous sensing of Hg^{2+} in water, soil and seafood and its application on test strips, *Anal. Chim. Acta*, 2018, **1023**, 105.

106 D. Xu, L. Tang, M. Tian, P. He and X. Yan, A benzothizole-based fluorescent probe for Hg^{2+} recognition utilizing ESIPT coupled AIE characteristics, *Tetrahedron Lett.*, 2017, **58**, 3654–3657.

107 T. Leng, Y. Ma and G. Chen, A novel ratiometric fluorescence and colorimetric probe with a large Stokes shift for Hg^{2+} sensing, *J. Photochem. Photobiol., A*, 2018, **353**, 143–149.

108 L. Huang, Z. Yang, Z. Zhou, Y. Li, S. Tang, W. Xiao, M. Hu, C. Peng, Y. Chen, B. Gu and H. Li, A dual colorimetric and

near-infrared fluorescent turn-on probe for Hg^{2+} detection and its applications, *Dyes Pigm.*, 2019, **163**, 118–125.

109 Y. Zhou, X. He, H. Chen, Y. Wang, S. Xiao, N. Zhang, D. Li and K. Zheng, An ESIPT/ICT modulation based ratiometric fluorescent probe for sensitive and selective sensing Hg^{2+}, *Sens. Actuators, B*, 2017, **247**, 626–631.

110 (*a*) Y. Y. Liu, S. Naha, N. Thirumalaivasan, S. Velmathi and S. P. Wu, A novel nanomolar highly selective fluorescent probe for imaging mercury (II) in living cells and zebrafish, *Sens. Actuators, B*, 2018, **277**, 673–678; (*b*) M. Tian, C. Wang, Q. Ma, Y. Bai, J. Sun and C. Ding, A Highly Selective Fluorescent Probe for Hg^{2+} Based on a 1, 8-Naphthalimide Derivative, *ACS Omega*, 2020, **5**, 18176–18184; (*c*) Z. Wang, Y. Zhang, J. Yin, Y. Yang, H. Luo, J. Song, X. Xu and S. Wang, A novel camphor-based ''turn-on'' fluorescent probe with high specificity and sensitivity for sensing mercury (II) in aqueous medium and its bioimaging application, *ACS Sustainable Chem. Eng.*, 2020, **8**, 12348–12359.

111 J. Shanmugapriya, S. Singaravadivel, G. Sivaraman and D. Chellappa, Anthracene-based highly selective and sensitive fluorescent ''turn-on'' chemodosimeter for Hg^{2+}, *ACS Omega*, 2018, **3**, 12341–12348.

112 S. L. Pan, K. Li, L. L. Li, M. Y. Li, L. Shi, Y. H. Liu and X. Q. Yu, A reaction-based ratiometric fluorescent sensor for the detection of Hg (ii) ions in both cells and bacteria, *Chem. Commun.*, 2018, **54**, 4955–4958.

113 C. Wu, J. Wang, J. Shen, C. Bi and H. Zhou, Coumarin-based Hg^{2+} fluorescent probe: Synthesis and turn-on fluorescence detection in neat aqueous solution, *Sens. Actuators, B*, 2017, **243**, 678–683.

114 M. Dong, J. Tang, Y. Lv, Y. Liu, J. Wang, T. Wang, J. Bian and C. Li, A dual–function fluorescent probe for Hg(II) and Cu(II) ions with two mutually independent sensing pathways and its logic gate behavior, *Spectrochim. Acta, Part A*, 2020, **226**, 117645.

115 Y. Chen, C. Yang, Z. Yu, B. Chen and Y. Han, A highly sensitive hemicyanine-based fluorescent chemodosimeter for mercury ions in aqueous solution and living cells, *RSC Adv.*, 2015, **5**, 82531–82534.

116 A. Gomathi and P. Viswanathamurthi, Near-infrared fluorogenic switches for the detection of Hg (II) ions: applications in real samples and living cells, *Anal. Methods*, 2019, **11**, 2769–2777.

117 B. Gu, L. Huang, N. Mi, P. Yin, Y. Zhang, X. Tu, X. Luo, S. Luo and S. Yao, An ESIPT-based fluorescent probe for highly selective and ratiometric detection of mercury(II) in solution and in cells, *Analyst*, 2015, **140**, 2778–2784.

118 C. Zhang, H. Zhang, M. Li, Y. Zhou, G. Zhang, L. Shi, Q. Yao, S. Shuang and C. Dong, A turn-on reactive fluorescent probe for Hg^{2+} in 100% aqueous solution, *Talanta*, 2019, **197**, 218–224.

119 Y. Gao, C. Zhang, S. Peng and H. Chen, A fluorescent and colorimetric probe enables simultaneous differential detection of Hg^{2+} and Cu^{2+} by two different mechanisms, *Sens. Actuators, B*, 2017, **238**, 455–461.

120 Y. Jiao, X. Liu, L. Zhou, H. He, P. Zhou and C. Duan, A Schiff-base dual emission ratiometric fluorescent chemosensor for Hg^{2+} ions and its application in cellular imaging, *Sens. Actuators, B*, 2017, **247**, 950–956.

121 Y. Li, S. Qi, C. Xia, Y. Xu, G. Duan and Y. Ge, A FRET ratiometric fluorescent probe for detection of Hg^{2+} based on an imidazo [1, 2-a] pyridine-rhodamine system, *Anal. Chim. Acta*, 2019, **1077**, 243–248.

122 Y. Ge, A. Liu, R. Ji, S. Shen and X. Cao, Detection of Hg^{2+} by a FRET ratiometric fluorescent probe based on a novel pyrido [1,2-a] benzimidazole-rhodamine system, *Sens. Actuators, B*, 2017, **251**, 410–415.

123 A. Tantipanjaporn, S. Prabpai, K. Suksen and P. Kongsaeree, A thiourea-appended rhodamine chemodosimeter for mercury(II) and its bioimaging application, *Spectrochim. Acta, Part A*, 2018, **192**, 101–107.

124 (*a*) C. G. Chen, N. Vijay, N. Thirumalaivasan, S. Velmathi and S. P. Wu, Coumarin-based Hg^{2+} fluorescent probe: Fluorescence turn-on detection for Hg^{2+} bioimaging in living cells and zebrafish, *Spectrochim. Acta, Part A*, 2019, **219**, 135–140; (*b*) G. Singh, P. Raj, H. Singh and N. Singh, Colorimetric detection and ratiometric quantification of mercury(II) using azophenol dye:'dip & read'based hand-held prototype device development, *J. Mater. Chem. C*, 2018, **6**, 12728–12738.

125 A. Malek, K. Bera, S. Biswas, G. Perumal, A. K. Das, M. Doble, T. Thomas and E. Prasad, Development of a next-generation fluorescent turn-on sensor to simultaneously detect and detoxify mercury in living samples, *Anal. Chem.*, 2019, **91**, 3533–3538.

126 A. Picard-Lafond, D. Lariviere and D. Boudreau, Revealing the hydrolysis mechanism of a Hg^{2+}-reactive fluorescein probe: Novel insights on thionocarbonated Dyes, *ACS Omega*, 2020, **5**, 701–711.

127 J. Xu, Z. Xu, Z. Wang, C. Liu, B. Zhu, X. Wang, K. Wang, J. Wang and G. Sang, A carbonothioate-based highly selective fluorescent probe with a large Stokes shift for detection of Hg^{2+}, *Luminescence*, 2018, **33**, 219–224.

128 D. Zhang, J. Liu, H. Yin, H. Wang, S. Li, M. Wang, M. Li, L. Zhou and J. Zhang, A Turn on ESIPT Probe for Rapid and Ratiometric Fluorogenic Detection of Hg^{2+} and its Application in Live-Cell Imaging, *J. Fluoresc.*, 2016, **26**, 1367–1372.

129 X. Duan, Z. Li, F. He and S. Wang, A sensitive and homogeneous SNP detection using cationic conjugated polymers, *J. Am. Chem. Soc.*, 2007, **129**, 4154–4155.

130 B. Liu and G. C. Bazan, Homogeneous fluorescence-based DNA detection with water-soluble conjugated polymers, *Chem. Mater.*, 2004, **16**, 4467–4476.

131 X. Cheng, Q. Li, J. Qin and Z. Li, A new approach to design ratiometric fluorescent probe for mercury (II) based on the Hg^{2+}-promoted deprotection of thioacetals, *ACS Appl. Mater. Interfaces*, 2010, **2**, 1066–1072.

132 S. Sarkar and R. Shunmugam, Polynorbornene derived 8-hydroxyquinoline paper strips for ultrasensitive chemical nerve agent surrogate sensing, *Chem. Commun.*, 2014, **50**, 8511–8513.

133 S. Sarkar, A. Mondal, A. K. Tiwari and R. Shunmugam, Unique emission from norbornene derived terpyridine-a selective chemodosimeter for G-type nerve agent surrogates, *Chem. Commun.*, 2012, **48**, 4223–4225.

134 S. Bhattacharya and R. Shunmugam, Unique norbornene based triazole molecule for selective Fe (II) sensing, *RSC Adv.*, 2015, **5**, 74973–74976.

135 J. Ding, H. Li, Y. Xie, Q. Peng, Q. Li and Z. Li, Reaction-based conjugated polymer fluorescent probe for mercury(II): good sensing performance with ''turn-on'' signal output, *Polym. Chem.*, 2017, **8**, 2221–2226.

136 U. Haldar and H. I. Lee, BODIPY-derived multi-channel polymeric chemosensor with pH-tunable sensitivity: selective colorimetric and fluorimetric detection of Hg^{2+} and HSO_4^- in aqueous media, *Polym. Chem.*, 2018, **9**, 4882–4890.

137 H. J. Kim and H. I. Lee, Thermo-tunable colorimetric detection of mercury (II) ions driven by the temperature-dependent assembly and disassembly of a block copolymer, *Polym. Chem.*, 2019, **10**, 4017–4024.

138 A. Balamurugan and H. I. Lee, Water-soluble polymeric probes for the selective sensing of mercury ion: pH-driven controllable detection sensitivity and time, *Macromolecules*, 2015, **48**, 1048–1054.

139 B. Wu, L. Xu, S. Wang, Y. Wang and W. Zhang, A PEGylated colorimetric and turn-on fluorescent sensor based on BODIPY for Hg (II) detection in water, *Polym. Chem.*, 2015, **6**, 4279–4289.

140 N. Choudhury, B. Saha, B. Ruidas and P. De, Dual-action polymeric probe: turn-on sensing and removal of Hg^{2+}; chemosensor for HSO_4^-, *ACS Appl. Polym. Mater.*, 2019, **1**, 461–471.

141 N. Choudhury, B. Ruidas, B. Saha, K. Srikanth, C. D. Mukhopadhyay and P. De, Multifunctional tryptophan-based fluorescent polymeric probes for sensing, bioimaging and removal of Cu^{2+} and Hg^{2+} ions, *Polym. Chem.*, 2020, **11**, 2015–2026.

142 (*a*) U. Haldar and H. I. Lee, BODIPY-derived polymeric chemosensor appended with thiosemicarbazone units for the simultaneous detection and separation of Hg (II) ions in pure aqueous media, *ACS Appl. Mater. Interfaces*, 2019, **11**, 13685–13693; (*b*) K. Chauhan, P. Singh and R. K. Singhal, New chitosan–thiomer: an efficient colorimetric sensor and effective sorbent for mercury at ultralow concentration, *ACS Appl. Mater. Interfaces*, 2015, **7**, 26069–26078.

143 S. Sirawatcharin, A. Saithongdee, A. Chaicham, B. Tomapatanaget, A. Imyim and N. Praphairaksit, Naked-eye and colorimetric detection of arsenic (III) using difluoroboron-curcumin in aqueous and resin bead support systems, *Anal. Sci.*, 2014, **30**, 1129–1134.

144 T. G. Akshay Krishna, V. Tekuri, M. Mohan and D. R. Trivedi, Selective colorimetric chemosensor for the detection of Hg^{2+} and arsenite ions using Isatin based Schiff's bases; DFT Studies and Applications in test strips, *Sens. Actuators, B*, 2019, **284**, 271–280.

145 S. Lohar, S. Pal, B. Sen, M. Mukherjee, S. Banerjee and P. Chattopadhyay, Selective and sensitive turn-on chemosensor for arsenite ion at the ppb level in aqueous media applicable in cell staining, *Anal. Chem.*, 2014, **86**, 11357–11361.

146 S. Paul, S. Bhuyan, S. K. Mukhopadhyay, N. C. Murmu and P. Banerjee, Sensitive and selective in vitro recognition of biologically toxic As (III) by rhodamine based chemoreceptor, *ACS Sustainable Chem. Eng.*, 2019, **7**, 13687–13697.

147 M. Baglan and S. Atılgan, Selective and sensitive turn-on fluorescent sensing of arsenite based on cysteine fused tetraphenylethene with AIE characteristics in aqueous media, *Chem. Commun.*, 2013, **49**, 5325–5327.

148 A. S. M. Islam, R. Alam, A. Katarkar, K. Chaudhuri and M. Ali, Di-oxime based selective fluorescent probe for arsenate and arsenite ions in a purely aqueous medium with living cell imaging applications and H-bonding induced microstructure formation, *Analyst*, 2015, **140**, 2979–2983.

149 K. Chauhan, P. Singh, B. Kumari and R. K. Singhal, Synthesis of new benzothiazole Schiff base as selective and sensitive colorimetric sensor for arsenic on-site detection at ppb level, *Anal. Methods*, 2017, **9**, 1779–1785.

150 M. L. Presti, S. El Sayed, R. Martínez-Máñez, A. M. Costero, S. Gil, M. Parra and F. Sancenon, Selective chromofluorogenic detection of trivalent cations in aqueous environments using a dehydration reaction, *New J. Chem.*, 2016, **40**, 9042–9045.

151 N. Yadav and A. K. Singh, Dual anion colorimetric and fluorometric sensing of arsenite and cyanide ions, *RSC Adv.*, 2016, **6**, 100136–100144.

152 R. Purkait, S. Maity and C. Sinha, A hydrazine-based thiocarbamide probe for colorimetric and turn-on fluorometric detection of PO_4^{3-} and AsO_3^{3-} in semi-aqueous medium, *New J. Chem.*, 2018, **42**, 6236–6246.

153 P. G. Sutariya, H. Soni, S. A. Gandhi and A. Pandya, Single-step fluorescence recognition of As^{3+}, Nd^{3+} and Br^- using pyrene-linked calix [4] arene: application to real samples, computational modelling and paper-based device, *New J. Chem.*, 2019, **43**, 737–747.

154 A. Deepa and V. Padmini, Highly Efficient Colorimetric Sensor for Selective and Sensitive Detection of Arsenite Ion (III) in Aqueous Medium, *J. Fluoresc.*, 2019, **29**, 813–818.

155 V. C. Ezeh and T. C. Harrop, A sensitive and selective fluorescence sensor for the detection of arsenic (III) in organic media, *Inorg. Chem.*, 2012, **51**, 1213–1215.

156 V. C. Ezeh and T. C. Harrop, Synthesis and properties of arsenic (III)-reactive coumarin-appended benzothiazolines: a new approach for Inorganic arsenic detection, *Inorg. Chem.*, 2013, **52**, 2323–2334.

157 S. Bhattacharya, S. Sarkar and R. Shunmugam, Unique norbornene polymer based ''in-field'' sensor for As (III), *J. Mater. Chem. A*, 2013, **1**, 8398–8405.